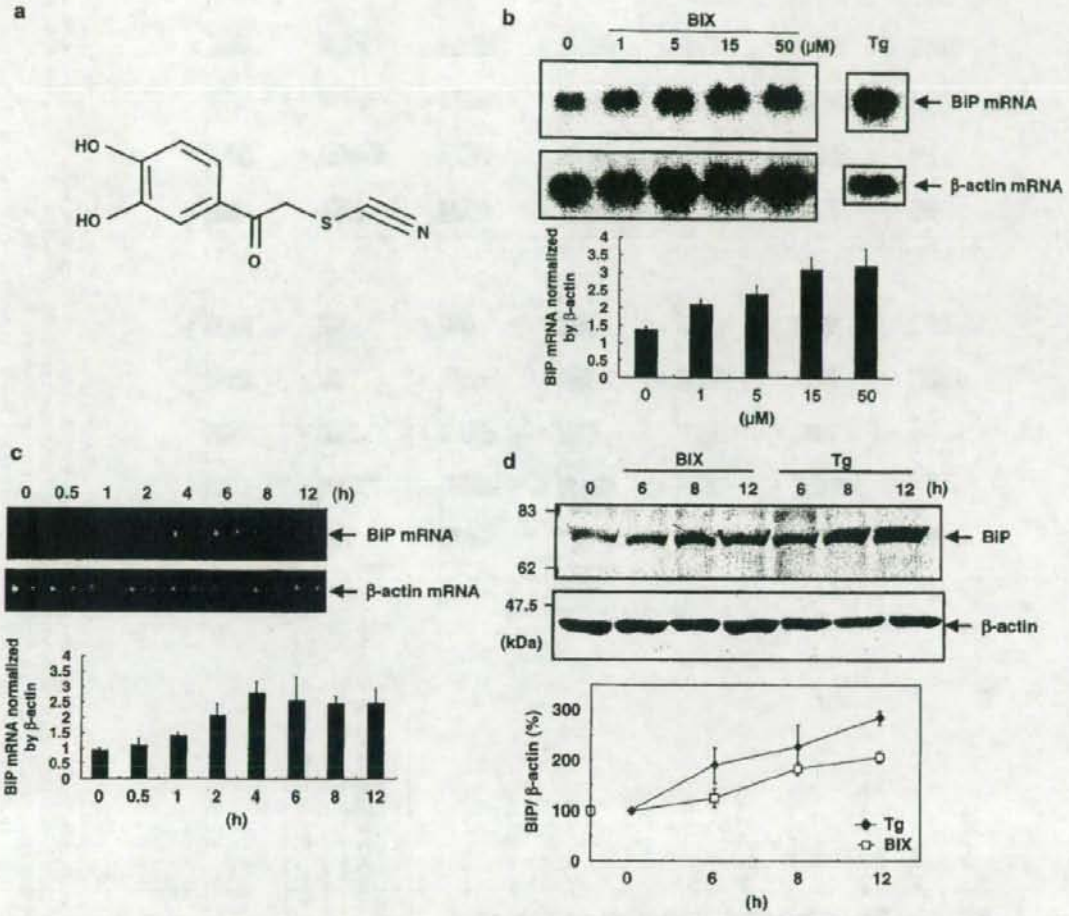

Figure 1 BIX induces BiP. (**a**) The structure of BIX (1-(3,4-dihydroxyphenyl)-2-thiocyanate-ethanone). (**b**) Dose-dependent induction of BiP mRNA in SK-N-SH cells after 6 h of treatment with BIX is shown by northern blot (upper panel) and real-time PCR (lower panel); values are means ± S.D. from three independent experiments. The induction of BiP mRNA by Tg is shown as a positive control. β-Actin mRNA is shown as an internal control. (**c**) The time course of BiP mRNA induction in cells treated with BIX is shown by semiquantitative RT-PCR (upper panel) and real-time PCR (lower panel); values are means ± S.D. from three independent experiments. The level of BiP mRNA peaked in 4 h and kept until 6 h after treatment with BIX at 5 μM, with a subsequent reduction after this point. (**d**) A time-dependent induction of BiP protein in SK-N-SH cells treated with 5 μM BIX or 1 μM Tg is detected by immunoblot and quantified by densitometry. Values are means ± S.D. from three independent experiments

finding supports the results shown in Figure 1c and suggests that the effects of BIX on BiP induction are transient and that BiP mRNA reverts to basal levels. Therefore, induction of BiP by BIX might be caused by a mechanism different to that used by ER stressors such as Tg and Tm, and the BIX-responsive element(s) might be included in the 132 bp BiP promoter region. Within this 132 bp region, there are three ER stress response elements (ERSEs) (Figure 3a). Subsequently, we carried out the reporter assay using an ERSE mut (132)-pGL3 plasmid (Figure 3a) to confirm whether or not these ERSEs are involved in the induction of BiP by BIX. BiP (132)-pGL3 or ERSE mut (132)-pGL3 was transfected into SK-N-SH cells, and the cells were treated with 5 μM BIX for 6 h. The reporter activities in cells transfected with BiP (132)-pGL3 were increased ~4-fold by BIX. On the other hand, induction of reporter activity was not observed in cells transfected with ERSE mut (132)-pGL3 (Figure 3c). This result suggests that ERSEs are involved in the induction of BiP by BIX.

Next, to examine whether three major transducers of the ER stress response, namely PERK, IRE1, and ATF6, affect the induction of BiP by BIX, we analyzed the expression of BiP in knockout/knockdown mouse embryonic fibroblasts (MEFs) lacking each transducer (Figure 3d). In PERK-deficient MEFs and IRE1α/β double-knockout MEFs, BiP mRNA was induced by BIX to a similar level to that seen in wild-type cells

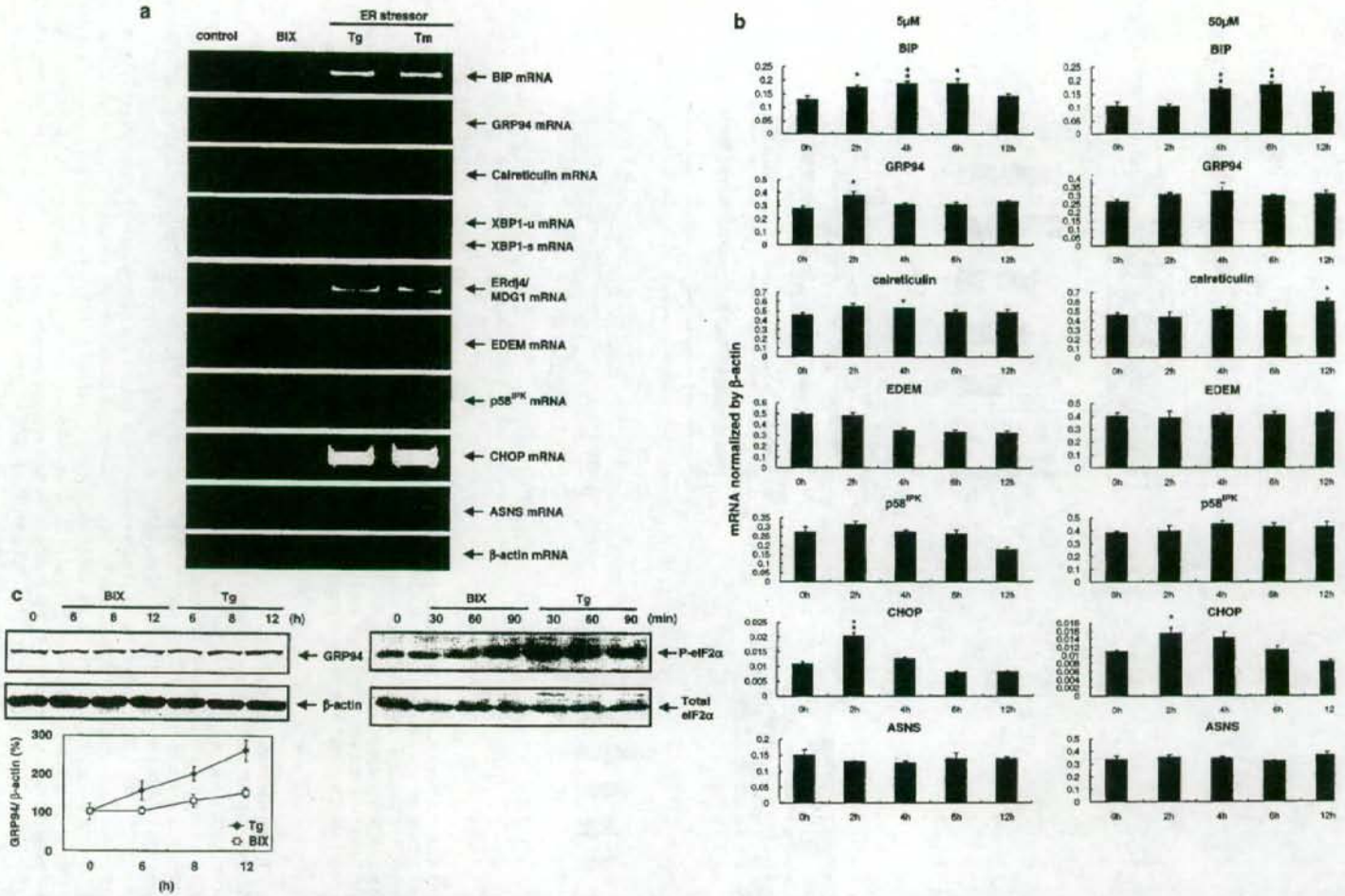

Figure 2 BIX preferentially induces BiP. (a) Semiquantitative RT-PCR analysis shows that a 6 h treatment of cells with 5 μM BIX induces BiP mRNA but not spliced XBP1 (XBP1-s), ERdj4/MDG1, EDEM, p58^{IPK}, and ASNS mRNAs, which are induced by 1 μM Tg or 1 μg/ml Tm. GRP94, calreticulin, CHOP are slightly induced by BIX. (b) Time-course analyses by real-time PCR show that 5 μM BIX significantly induces BiP from 2 to 6 h after BIX administration and transiently induces GRP94, calreticulin, and CHOP. The mRNAs of EDEM, p58^{IPK}, and ASNS are not changed from 2 to 12 h. A 50 μM portion of BIX also induces BiP from 4 to 6 h and transiently induces calreticulin and CHOP. Even 50 μM BIX does not induce EDEM, p58^{IPK}, and ASNS. Values are means ± S.E. from 3–4 independent experiments. Significant differences are based on the values at 0 h, $^{*}P<0.05$, $^{**}P<0.01$. (c) Immunoblot analysis with quantification shows that 5 μM BIX causes very slight induction of GRP94 protein but does not induce the phosphorylation of eIF2α at any time point, compared with 1 μM Tg. Values are means ± S.D. from three independent experiments

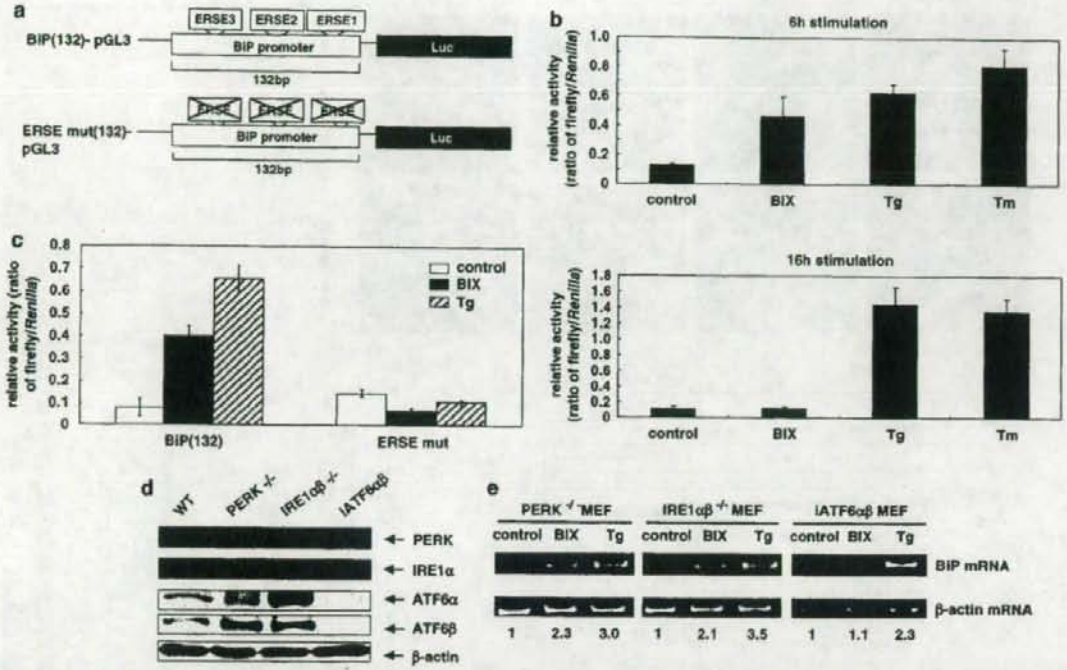

Figure 3 The induction of BiP by BIX is mediated by ERSE and the ATF6 pathway. (**a**) Schematic representation of the BiP promoter cloned into the pGL3 plasmid (BiP (132)-pGL3) and the ERSE mutant BiP promoter cloned into the pGL3 plasmid (ERSE mut (132)-pGL3). (**b**) The luciferase activities driven by the BiP promoter are normalized against *Renilla* luciferase activities. The induction of luciferase activity in BiP (132)-pGL3-transfected cells that are treated with 5 μM BIX increased at 6 h after BIX treatment and reversed to basal levels by 16 h. Induction of luciferase activity in 300 nM Tg- or 0.5 μg/ml Tm-treated cells is sustained until 16 h after BIX treatment. Values are means ± S.D. from five independent experiments. (**c**) The relative reporter activity in cells transfected with BiP (132)-pGL3 (ratio of firefly/*Renilla*) at 6 h after treatment in cells treated with BIX (5 μM) are increased ~4-fold, whereas that in cells transfected with ERSE mut (132)-pGL3 are not increased. Values are means ± S.D. from five independent experiments. Tg (300 nM) also increases reporter activity in cells transfected with BiP (132)-pGL3, but not in cells transfected with mut (132)-pGL3. (**d**) Immunoblot analyses of PERK$^{-/-}$ MEFs, IRE1$\alpha\beta^{-/-}$ MEFs, and iATF6$\alpha\beta$ (knockdown) MEFs with anti-PERK, anti-IRE1 and anti-ATF6α/β antibodies prove the deficiency of those genes. (**e**) Semiquantitative RT-PCR analysis shows that BiP mRNA is induced at 6 h after treatment with BIX (50 μM) in PERK$^{-/-}$ MEFs and IRE1$\alpha\beta^{-/-}$ MEFs, but not in iATF6$\alpha\beta$ (knockdown) MEFs. Tg induces BiP mRNA in all three MEFs. Numeric values below the panels indicate the induction ratio of BiP mRNA adjusted to the level of β-actin mRNA with reference to non-treated control sample as one

(Figure 3e). These results indicate that the induction of BiP by BIX is not mediated via the PERK or IRE1 pathways. The data showing that eIF2α is not phosphorylated by BIX (Figure 2c), and that XBP1 is not processed by BIX (Figure 2a), support this conclusion. By contrast, BiP was not induced by BIX in ATF6$\alpha\beta$ double-knockdown MEFs (Figure 3e), suggesting that BIX treatment mediates the induction of BiP via the ATF6 pathway. These results were also obtained by northern blot analysis (data not shown). The data showing that BIX induced GRP94, calreticulin, and CHOP, and that ERdj4/MDG1, EDEM, p58^{IPK} and ASNS were not induced by BIX (Figure 2a, b), also suggested that the effect of BIX is mediated by the ATF6 pathway. This is because the inductions of GRP94, calreticulin, and CHOP are known to be dependent on the activation of ATF6; inductions of ERdj4/MDG1, EDEM, p58^{IPK} are known to be mediated by IRE1 and that of ASNS by PERK. Next, we tried to detect the cleavage of ATF6 in cells treated with BIX, but we have not yet detected cleaved N-terminal fragments of endogenous ATF6 using the antibody described in this study (data not shown).

BIX protects SK-N-SH cells from ER stress-induced apoptosis. BiP functions as a cytoprotective protein in stressed cells.[14–16] As BIX activates BiP expression, BIX might protect cells from ER stress. To investigate whether BIX has the ability to prevent apoptosis induced by ER stress, SK-N-SH cells were pretreated for 12 h with 0 or 5 μM BIX, which was then replaced with fresh medium containing 0.5 μg/ml Tm. Phase-contrast images (Figure 4a–d) and fluorescence micrographs (Figure 4e–h) of Hoechst staining show that apoptotic cell death was observed within 36 h of Tm treatment (Figure 4d, h), and that the number of dead cells had increased significantly (Figure 4i). By contrast, cell death was significantly inhibited by pretreatment with BIX (Figure 4c, g, i). We also found that treatment of cells with BIX only for 36 h caused no changes in cells (Figure 4b, f). Next, we looked at the activation of caspases 4 and 3/7 after ER stress. Caspase 4 was reported to be activated in response to ER stress in human cells.[5] Immunoblot analysis showed that pretreatment of cells with BIX attenuated the cleavage of caspase 4 (Figure 4j). Moreover, we analyzed

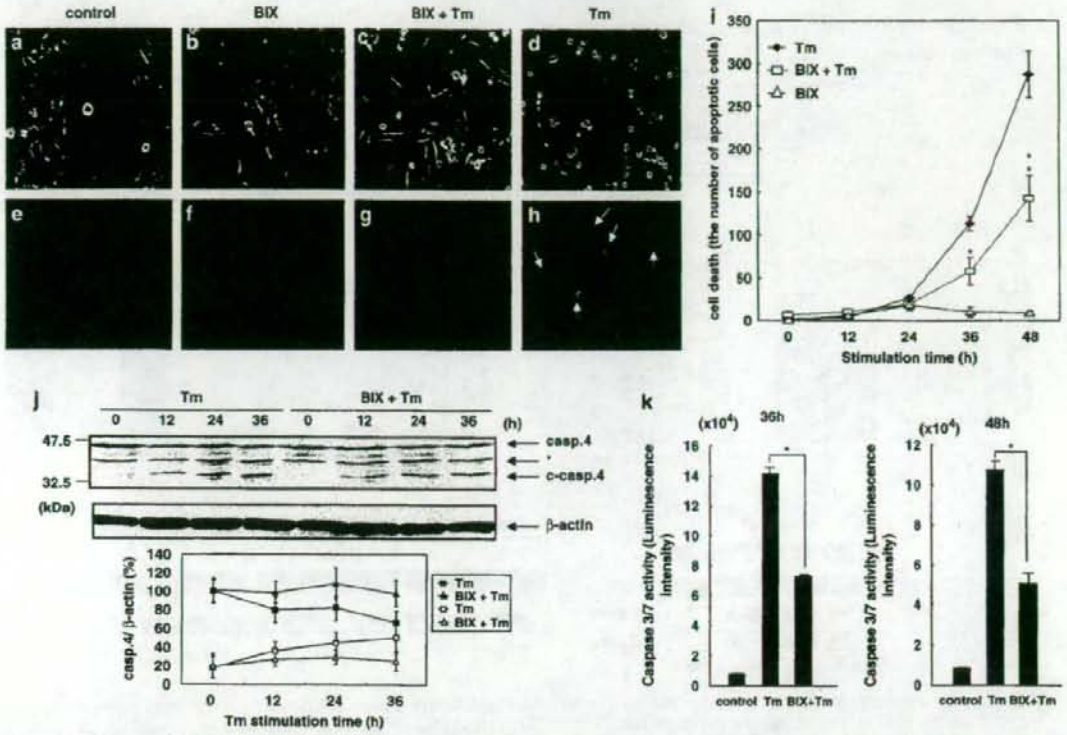

Figure 4 BIX protects SK-N-SH cells from ER stress-induced apoptosis. SK-N-SH cells are pretreated with vehicle (control: **a**, **e**; Tm: **d**, **h**) or with 5 μM BIX (BIX: **b**, **f**; BIX + Tm: **c**, **g**) for 12 h, and then the whole medium is replaced with fresh medium (control, BIX) or medium supplemented with 0.5 μg/ml Tm (BIX + Tm, Tm). Phase-contrast images (**a**–**d**) and fluorescence micrographs of Hoechst staining (**e**–**h**) at 36 h after Tm stimulation show that pretreatment of cells with BIX reduces the number of Tm-induced apoptotic cells. Arrows show apoptotic cells (**h**). (**i**) The number of dead cells (apoptotic cells) after Tm treatment increases from 0 to 48 h. Pretreatment of cells with BIX significantly reduces the amount of cell death compared with cells treated with Tm only (*$P<0.05$, **$P<0.01$). BIX alone does not cause remarkable cell death. A total of 500 cells are counted at each time point. Values are means ± S.D. from five independent experiments. (**j**) Immunoblot of caspase 4 shows that Tm causes cleavage of caspase 4 (c-Casp.4) in a time-dependent manner and that pretreatment of cells with BIX attenuates this cleavage with no change in the level of β-actin. Asterisk indicates nonspecific bands. The lower panel shows quantitative analyses of full-length and cleaved caspase 4. Filled square and triangle indicate full-length caspase 4; open square and triangle indicate cleaved caspase 4. Values are means ± S.D. from three independent experiments. (**k**) The caspases 3 and 7 activities in Tm-treated cells are increased. BIX reduces this caspase activity to almost half value of the Tm-treated levels. Values are means ± S.D. from three independent experiments; *$P<0.01$

the activities of caspases 3 and 7. The activities of caspases 3 and 7 in Tm-treated cells were extremely high. By contrast, BIX reduced the activities of caspases 3 and 7 to half of those in cells treated with Tm only (Figure 4k). Taken together, these findings suggest that pretreatment of cells with BIX inhibits cell death induced by ER stress involving inhibited activation of caspases 3/7 and 4.

BIX administration reduces the insults due to cerebral infarction. Because it has been shown that cerebral ischemia causes ER stress,[20] we performed occlusions of the middle cerebral arteries (MCAs) of mice to confirm whether the protective effects of BIX *in vitro* can be utilized *in vivo*. Immunoblot analysis of extracts from the cerebral hemisphere showed that 20 μg (2 μl) of BIX (administered intracerebroventricularly) significantly increased the level of BiP protein 24 h after administration, confirming that administration of BIX induces BiP protein *in vivo* (Figure 5a). Real-time PCR analysis of the expression of ER stress response-related genes showed that 20 μg BIX significantly induced BiP at 6 h after administration (Figure 5b). The levels of GRP94, calreticulin, and CHOP mRNA also increased; however, those of EDEM, p58^{IPK}, and ASNS did not change (Figure 5b), consistent with the results of *in vitro* study (Figure 2b). Animals treated with BIX showed no behavioral changes, except for the neurological deficits induced by ischemia. Neurological evaluation at 24 h after MCA occlusion showed that most of the vehicle-administered (control) mice presented with moderate symptoms; for example, circling to the contralateral side (Figure 5c). By contrast, most BIX-administered (5 or 20 μg) mice presented with milder symptoms; for example, extending the right forepaw (Figure 5c).

Twenty-four hours after occlusion, 2,3,5-triphenyltetrazolium chloride (TTC) staining showed that the mice had developed infarcts affecting the ipsilateral cortex and striatum

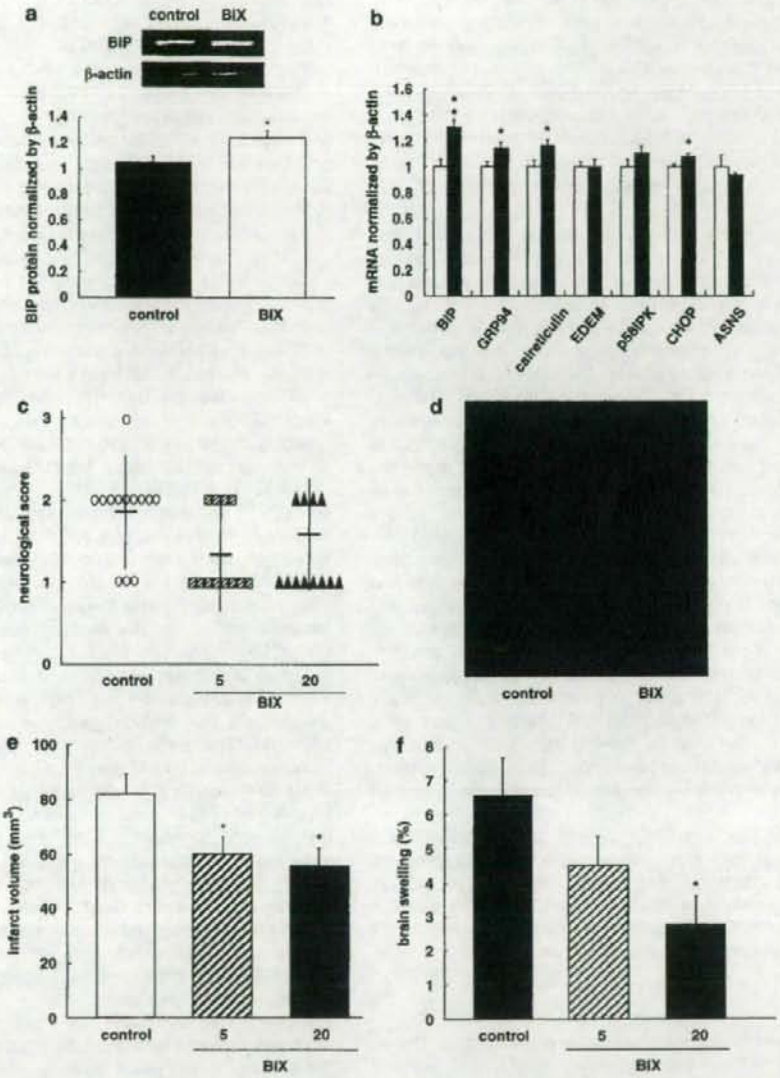

Figure 5 BIX administration reduces the extent of cerebral infarction after MCA occlusion. (**a**) It is confirmed that intracerebroventricular administration of BIX raises the level of BiP protein in mouse brains. Immunoblot analysis of BiP and β-actin protein in BIX-administered (20 μg/2 μl) brains shows that the level of BiP protein is significantly increased at 24 h after BIX administration compared with vehicle-treated brains. The inset is the representative immunoblot detected by luminescence of ECL. Densitometric scanning of BiP bands normalized to β-actin was performed. Data are represented as means ± S.E. from four independent experiments; $^{*}P<0.05$. (**b**) The real-time PCR shows that the level of BiP (in arbitrary units) in the BIX-administered (20 μg/2 μl) hemisphere is increased significantly at 6 h after administration. The levels of GRP94, calreticulin, and CHOP mRNA are increased by BIX; the levels of EDEM, p58^{IPK}, and ASNS do not change. The black bar is the BIX-administered (20 μg/2 μl) hemisphere; the white bar is the vehicle-administered hemisphere. Values are means ± S.E. from 3–4 independent experiments; $^{*}P<0.05$, $^{**}P<0.01$. (**c**) Neurological deficits at 24 h after occlusion of the MCA are scored using the following scale: 0 = no observable neurological deficits (normal); 1 = failure to extend the right forepaw (mild); 2 = circling to the contralateral side (moderate); 3 = loss of walking or righting reflex (severe). BIX administration (5 or 20 μg) improves neurological deficits induced by MCA occlusion. Values are means (horizontal bold bar) ± S.D. (**d**) Representative images of TTC staining at 24 h after MCA occlusion. Note that the infarct area (white or pink) in BIX-administered brains is smaller than that in brains treated with vehicle. (**e**) Quantitative analysis of infarct volumes measured by TTC staining. Values are means ± S.E. from 12 or 13 independent experiments; $^{*}P<0.05$. (**f**) BIX administration (5 or 20 μg) reduces brain swelling induced by MCA occlusion. Values are means ± S.E. from 12 or 13 independent experiments; $^{*}P<0.05$

(Figure 5d). The core of infarction was observed as a white area and the penumbra was pink. The infarction area (core + penumbra) observed in BIX-treated brains was smaller than that in vehicle-treated brains (Figure 5d). Quantitation of TTC staining showed that administration of 5 or 20 μg of BIX significantly reduced the infarction area (Figure 5e). Furthermore, measurement of brain swelling also showed that administration of 20 μg of BIX significantly reduced brain swelling after 24 h of ischemia (Figure 5f).

BIX administration reduces apoptosis induced in the penumbra by MCA occlusion. Detailed observation of TTC-stained ischemic brains indicated that the reduction in the area of infarction in BIX-treated brains was predominantly due to a reduction in the area of the penumbra rather than the core. Therefore, we examined the penumbra of BIX-treated brain for evidence of apoptosis. Terminal deoxynucleotidyl transferase-mediated dUTP–biotin nick end labeling (TUNEL) staining of ischemic brains without BIX treatment revealed an increased number of TUNEL-positive cells in the ipsilateral core and penumbra compared with the contralateral side (Figure 6a). By contrast, the number of TUNEL-positive cells was significantly reduced in the ipsilateral penumbra of BIX-treated brains compared with that of vehicle-treated brains (Figure 6a, b). Immunohistochemistry for caspase 3 in the penumbrae of BIX- and vehicle-treated brains showed that BIX reduced the number of apoptotic cells at 24 h after MCA occlusion (Figure 6c, d). CHOP plays a role in apoptotic cell death by ER stress.[21] Moreover, it is well-known that CHOP is induced after ischemic insults.[22] Therefore, we examined the effects of BIX treatment on the induction of CHOP mRNA after ischemia. *In situ* hybridization analysis showed that CHOP mRNA was significantly induced in the penumbra of MCA-occluded mice, whereas pretreatment of mice with BIX resulted in a marked reduction in the level of CHOP mRNA expression (Figure 6e, f). Although BIX induced CHOP (Figure 5b), the extent of this induction was very weak compared with the expression induced by ischemia (Figure 6e, f). The results of TUNEL staining and *in situ* hybridization for CHOP indicate that BIX suppresses the ER stress-mediated apoptotic cell death induced in the penumbra after ischemia.

Discussion

If a BiP inducer is just an ER stressor such as Tg or Tm, its application as a therapeutic strategy is unlikely to be realized because it may activate several pathways of the UPR, including ER stress-induced apoptotic pathways. The present studies in knockout or knockdown MEFs deficient in ER stress sensors showed that the ATF6 pathway is necessary for BIX to induce BiP. This is consistent with the evidence that BIX preferentially induced BiP with slight inductions of GRP94, calreticulin, and CHOP mediated by the ATF6 pathway, and that BIX does not affect the pathway downstream of IRE1 or the translational control branch downstream of PERK. Moreover, for the apoptotic branches of ER stress, the transient induction of CHOP by BIX was very weak compared with the severe induction observed in ER stress, and caspase 4 was not activated by BIX. The differences among inductions between BiP and the other genes of the ATF6 pathway by BIX suggested that elements other than ERSEs may be involved in the induction of BiP by BIX.

The present data from *in vitro* studies showed that BIX suppresses the cleavage of caspase 4, a member of one of the apoptotic pathways mediated by ER stress. Because it was reported that PERK is activated after cerebral ischemia[10] and that XBP1 mRNA splicing is detected after transient cerebral ischemia,[11] it would appear that cerebral ischemia causes ER stress. Thus, to examine the antiapoptotic effect of BIX *in vivo*, we used MCA-occluded mice. Intracerebroventricular pretreatment of mice with BIX reduced the area of infarction in the brain, especially the area of the penumbra. BIX pretreatment also reduced the severity of neurological deficits caused by focal cerebral ischemia. In the penumbrae of BIX-treated brains, the induction of CHOP, an apoptotic molecule induced by ER stress, was suppressed, suggesting that BIX reduces cell death by preventing ER stress-induced apoptosis. As the infarct volumes, brain swelling, and neurological scores following 5 and 20 μg treatments were similar, 5 μg of BIX might be sufficient to protect against ischemia. This is the first report demonstrating the *in vivo* success of a therapeutic manipulation to inhibit apoptosis mediated by ER stress, indicting that BIX might be a potential therapeutic for neuroprotection after cerebral infarction.

The induction of BiP by BIX was transient, peaking at 4 h after treatment, but the levels of BiP protein continued to increase until 12 h. The reporter assay using the 132 bp BiP-pGL3 plasmid also showed that the effect of BIX on the induction of BiP was transient and weaker than the effect of ER stressors, such as Tg or Tm. Even a high dosage of BIX (50 μM) did not induce genes mediated by non-ATF6 pathways. These results imply that the mechanism of BiP induction utilized by BIX may be different from those used by these ER stressors. It was reported that the activation of transducers of ER stress is caused by dissociation of BiP from their luminal domains.[23] It may be assumed that artificial induction of BiP disturbs the activation of transducers of ER stress, because abundant BiP remains bound to these transducers preventing their activation. However, the effect of BIX peaked at 4 h and remained at that level until 6 h after treatment; after this point, there was a subsequent reduction in level. Therefore, the production of BiP induced by BIX may not disturb this dissociation.

An earlier study showed that a selective inhibitor of eIF2α dephosphorylation protects cells from ER stress[12] and that the development of novel chemical compounds for diseases related to ER stress is underway. It is possible that BIX, which has effects *in vivo*, could have therapeutic applications in the treatment of diseases involving ER stress. We propose that BiP activators, such as BIX, will be effective agents against ER stress. However, further studies will be required to investigate the pharmacology of BIX, including its possible side effects, before BiP activators can be used in clinical practice.

Materials and Methods

Cell culture. SK-N-SH neuroblastoma cells were grown in α-modified Eagle's medium supplemented with 10% fetal bovine serum. MEFs derived from IRE1$^{-/-}$ embryos or PERK$^{-/-}$ embryos were cultured in Dulbecco's modified Eagle's

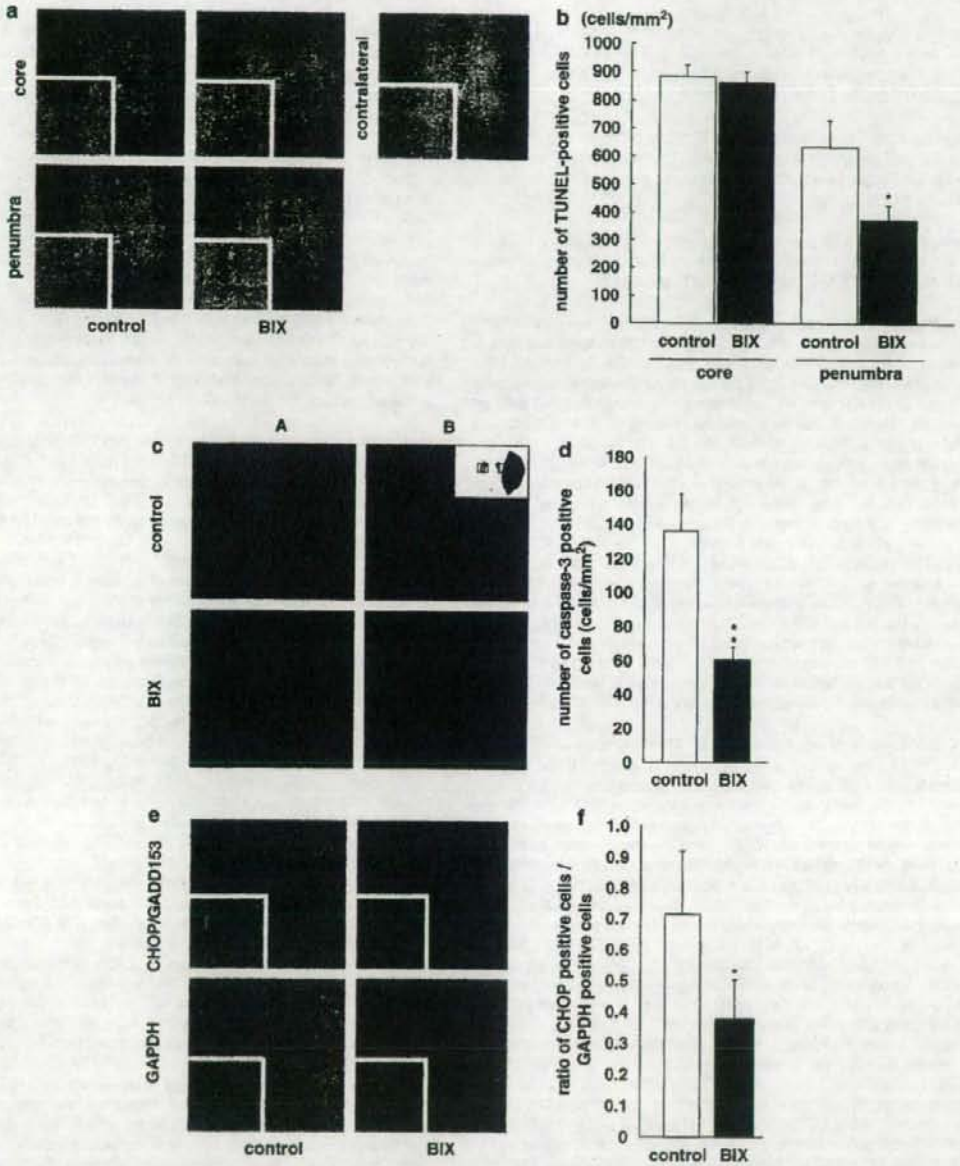

Figure 6 A 20 μg portion of BIX administration reduces ER stress-induced apoptosis induced in the penumbra by MCA occlusion. (**a**) Representative images of TUNEL staining in the core, penumbra, or contralateral side to the infarction at 24 h. Insets are higher magnification images. BIX administration reduces the number of TUNEL-positive cells induced in the penumbra by MCA occlusion. Scale bar for higher magnification panels, 10 μm; lower magnification panels, 100 μm. (**b**) Cell-counting analysis shows that BIX significantly reduced the number of TUNEL-positive cells in the penumbra. Values are means ± S.D. from 9 or 10 independent experiments; $^{*}P<0.05$. (**c**) Representative image showing immunohistochemical staining for caspase 3 in the penumbra area (**A**) and contralateral area (**B**) in a BIX-treated mouse and vehicle-treated mouse at 24 h after treatment. Scale bar, 50 μm. (**d**) Quantitative analysis of caspase 3-positive cells. Values shown are the number of caspase 3-positive cells/mm^2. Values are means ± S.D. from five independent experiments; $^{**}P<0.01$. (**e**) Representative images of *in situ* hybridization for CHOP, an apoptotic molecule induced in penumbra by ER stress at 24 h. Insets are higher magnification images. Scale bar for higher magnification panels, 10 μm; lower magnification panels, 100 μm. (**f**) Quantitative analysis of CHOP-positive cells. Values shown are the ratios of CHOP-/GAPDH-positive cells. Values are means ± S.D. from five independent experiments; $^{*}P<0.05$

medium supplemented with 10% fetal bovine serum. MEFs in which both ATF6α and ATF6β (iATF6αβMEF) had been knocked down were also maintained in the Dulbecco's modified Eagle's medium. PERK$^{-/-}$ MEFs, IRE1$^{-/-}$ MEFs, and iATF6αβMEFs were kindly provided by Drs. David Ron (New York University, NY, USA), Dr. Fumihiko Urano (University of Massachusetts Medical School, MA, USA), and Laurie H Glimcher (Harvard School of Public Health, MA, USA), respectively.

Reagents. Cells were treated with Tm or Tg to induce ER stress conditions. Tm was purchased from Sigma (St. Louis, MO, USA). Tg was purchased from Alomone Labs Ltd (Jerusalem, Israel). Hoechst staining was performed according to the manufacturer's instructions.

Plasmids. A pGL3-BiP promoter (132)-Luc reporter plasmid (BiP (132)-pGL3) and an ERSE mutant BiP promoter-Luc reporter plasmid (ERSE mut (132)-pGL3) were provided by Dr. K Mori (Kyoto University, Kyoto, Japan).

Transfection and reporter assays. SK-N-SH cells were grown to 80% confluence and then transfected using Lipofectamine 2000 reagent, according to the manufacturer's instructions (Invitrogen, Carlsbad, CA, USA). Cells were transfected with a reporter plasmid (0.2 μg) carrying the firefly luciferase gene under the control of the BiP promoter, and a reference plasmid pRL-SV40 (0.02 μg) carrying the *Renilla* luciferase gene under the control of the SV40 enhancer and promoter (Promega, Madison, WI, USA). At 12 h after transfection, cells were treated with library compounds to screen for compounds that induce BiP. Firefly and *Renilla* luciferase activities were measured in 10 μl of cell lysate using a Dual-Luciferase Reporter Assay System (Promega) and a luminometer (Berthold Technologies, Bad Wildbad, Germany). Relative luciferase activity was defined as the ratio of firefly luciferase activity to *Renilla* luciferase activity. Values were averaged from quadruplicate determinations. Using these BiP reporter cells, HTS was performed on a compound library consisting of approximately 10 000 compounds. The molecules were synthesized based on the structures of 10 lead compounds that had high activity in HTS. Among the synthesized molecules, we chose a small molecule that had the highest activity, naming it BIX. To confirm the induction of BiP by this compound, 5 μM BIX, 300 nM Tg or 0.5 μg/ml Tm were added to cell and the luciferase assay was performed as described; luciferase activities were measured in three independent experiments.

RNA isolation and semiquantitative RT-PCR analysis. SK-N-SH cells or MEFs were washed with phosphate-buffered seline (PBS) and then collected by centrifugation. Total RNA was isolated from cells using an RNeasy kit (Qiagen, Tokyo, Japan) according to the manufacturer's protocol. Total RNA was isolated from frozen brains using the acid guanidine–phenol–chloroform RNA extraction method provided as ISOGEN (Nippon Gene, Toyama, Japan), and purified using an RNeasy Mini kit (Qiagen). RNA concentrations were determined spectrophotometrically at 260 nm. First-strand cDNA was synthesized in a 20-μl reaction volume using a random primer (Takara, Shiga, Japan) and Moloney murine leukemia virus reverse transcriptase (Invitrogen). PCR was performed in a total volume of 30 μl containing 0.8 μM of each primer, 0.2 mM dNTPs, 3 U *Taq* DNA polymerase (Promega), 2.5 mM $MgCl_2$, and 1 × PCR buffer. The amplification conditions for semiquantitative RT-PCR analysis were as follows: an initial denaturation step of 95°C for 5 min, 22 cycles of 95°C for 1 min, 55°C for 1 min, and 72°C for 1 min, and a final extension step of 72°C for 7 min. The numbers of amplification cycles for detection of BiP and β-actin were 18 and 15, respectively. The primers used for amplification were as follows: BiP: 5′-GTTTGCTGAGG AAGACAAAAAGCTC-3′ and 5′-CACTTCCATAGAGTTTGCTGATAATTG-3′; XBP1: 5′-CAGCGCTTGGGGATGGATGC-3′ and 5′-CCATGGGGAGATGTTCTG GA-3′; CHOP: 5′-GGAGCTGGAAGCCTGGTATGAGG-3′ and 5′-TCCCTGGTCA GGCGCTCGATTTCC-3′; GRP94: 5′- CTCACCATTTGGATCCTGTGTG-3′ and 5′-CACATGACAAGATTTTACATCAAGA-3′; calreticulin: 5′-GCCAAGGACGAGCT GTAGAGAG-3′ and 5′-GGTGAGGGCTGAAGGAGAATC-3′; ERdj4/MDG1: 5′-TCTAGAATGGCTACTCCCCAGTCAATTTTC-3′ and 5′-TCTAGACTACTGTCCT GAACAGTCAGTG-3′; EDEM: 5′-TGGGTTGGAAAGCAGAGTGGC-3′ and 5′-TCCATTCCTACATGGAGGTAG-3′; $p58^{IPK}$ 5′-GAGGTTTGTGTTTGGGATGCAG-3′ and 5′-GCTCTTCAGCTGACTCAATCAG-3′; ASNS: 5′-AGGTTGATGATGCAATG ATGG-3′ and 5′-TCCCCTATCTACCCACAGTCC-3′; β-actin: 5′-TCCTCCCTGGA GAAGAGCTAC-3′ and 5′-TCCTGCTTGCTGATCCACAT-3′. PCR products were resolved by electrophoresis through 4.8% (w/v) polyacrylamide gels. The density of each band was quantified using the Scion Image Program (Scion Corporation, Frederick, MD, USA).

Northern blot analysis. Total RNA (10 μg/lane) was resolved by electrophoresis through 1.0% agarose/formaldehyde gels and transferred onto Immobilon-NY + membranes (Millipore, Bedford, MA, USA). Filters were hybridized with ^{32}P-labeled cDNA probes generated from the BiP cDNA by the Random Primer DNA labeling kit (Takara). After washing in 2 × SSC/0.1% SDS and 0.1 × SSC/0.1% SDS, filters were exposed onto IP plates (Fuji Film, Tokyo, Japan) and analyzed using a BAS1800 system (Fuji Film).

Real-time PCR. TaqMan real-time PCR was performed as described previously.[24] Single-stranded cDNA was synthesized from total RNA using a High-Capacity cDNA Archive Kit (Applied Biosystems, Foster City, CA, USA). Quantitative real-time PCR was performed using an ABI PRISM® 7900HT Sequence Detection System (Applied Biosystems) with a TaqMan Universal PCR Master Mix (Applied Biosystems) according to the manufacturer's protocol. The expressions of mRNAs were measured by real-time PCR using the Applied Biosystems Assays-on-Demand™ Gene Expression Product. The thermal cycler conditions were as follows: 2 min at 50°C and then 10 min at 95°C, followed by two-step PCR for 50 cycles consisting of 95°C for 15 s followed by 60°C for 1 min. For each PCR, we checked the slope value, R^2 value, and linear range of a standard curve of serial dilutions. All reactions were performed in duplicate. The results are expressed relative to the β-actin, internal control.

Immunoblot analysis. Cells were washed with PBS, harvested and lysed in Nonidet P-40 lysis buffer (1% Nonidet P-40, 20 mM HEPES (pH 7.6), 100 mM NaCl, 3 mM $MgCl_2$, 5 mM dithiothreitol, and 0.1% protease inhibitor cocktail (Sigma)). Lysates were then sonicated on ice three times for 5 s and centrifuged at 15 000 r.p.m. for 5 min. Supernatants were retained and boiled for 5 min in SDS sample buffer. Equal amounts of protein were subjected to 10–15% SDS-PAGE, transferred to PVDF membranes, and immunoblotted with each primary antibody. Membranes were washed with TBS/Tween-20, and then incubated with an alkaline phosphatase-conjugated secondary antibody (Sigma). The corresponding bands were detected using ECL Plus Western Blotting Detection System (GE Healthcare UK Ltd, Buckinghamshire, England). The density of each band was quantified using the Scion Image Program (Scion Corporation). As primary antibodies, anti-PERK antibody was provided by Dr. David Ron (New York University) and anti-IRE1α antibody was provided by Dr. Fumihiko Urano (University of Massachusetts Medical School). Anti-KDEL (Stressgen, Victoria, BC, Canada), anti-total eIF2α (Cell signaling Technology, Beverly, MA, USA), anti-eIF2α (phosphospecific) (Stressgen), anti-ATF6α (Santa Cruz Biotechnology, Santa Cruz, CA, USA), anti-ATF6β (Santa Cruz Biotechnology), anti-TX (MBL Co. Ltd, Nagoya, Japan), and anti-actin (Chemicon, Temecula, CA, USA) antibodies were purchased commercially. Anti-KDEL antibody detected BiP and GRP94. Anti-TX antibody detected caspase 4 protein.

Caspase activity. SK-N-SH cells were seeded into 96-well culture plates (1.0×10^4 cells/well). Cells were cultured under standard conditions for 12 h, and then treated with 5 μM BIX or vehicle for another 12 h. After BIX or vehicle treatment, the whole medium was replaced with fresh medium containing 0.5 μg/ml Tm and cells were incubated for additional 36 or 48 h. After incubation, caspase-3 and -7 activity was measured using a caspase-Glo 3/7 Assay kit (Promega), according to the manufacturer's instructions. Luminescent signals were measured using a luminometer (Berthold Technologies). The measurement of caspases 3 and 7 activities was conducted in three independent experiments.

Cell death assay. SK-N-SH cells were pretreated with 5 μM BIX or vehicle for 12 h, after which the whole medium was replaced with fresh medium containing 0.5 μg/ml Tm, in which cell were cultured for the indicated times. Cells were fixed with 4% paraformeldehyde for 30 min at 4°C, washed with PBS for 5 min, and then stained with 100 μM Hoechst 33258 (Wako Pure Chemical Co., Tokyo, Japan) in PBS for 20 min. A total of 500 cells were counted randomly and apoptotic cells were determined by fluorescence microscopy.

Focal cerebral ischemia model in mice. Male adult ddY mice weighing 24–34 g (Japan SLC) were used in experiments, and were housed under diurnal lighting conditions. Anesthesia was induced by 2.0% isoflurane, then maintained using 1% isoflurane in 70% N_2O and 30% O_2 using an animal general anesthesia machine (Soft Lander, Sin-ei Industry Co. Ltd, Saitama, Japan). Body temperature was maintained between 37.0 and 37.5°C with the aid of a heating pad and heating lamp. A filament occlusion of the left MCA was carried out as previously

described.[25,26] Briefly, the left MCA was occluded with an 8-0 nylon monofilament (Ethicon, Somerville, NJ, USA) coated with a mixture of silicone resin (Xantopren; Bayer Dental, Osaka, Japan). This coated filament was introduced into the internal carotid artery through the common carotid artery up to the origin of the anterior cerebral artery, so as to occlude the MCA and posterior communicating artery. At the same time, the left common carotid artery was occluded by the suture. Permanent ischemia was selected because it produced a reproducible subtotal infarction in our previous studies.[25,26] Twenty-four hours after the occlusion, the forebrain was divided into five coronal 2 mm sections using a mouse brain matrix (RBM-2000C; Activational Systems, Warren, MI, USA). Sections were then stained with 2% TTC. Images of the infarcted areas were recorded using a digital camera (Nikon, COOLPIX4500), quantitated using Image J software (http://rsb.info.nih.gov/ij/download/), and calculated as in a previous report.[26] Brain swelling was calculated according to the following formula: (infarct volume + ipsilateral undamaged volume−contralateral volume) × 100/contralateral volume (%).[25] BIX was dissolved in 10% DMSO and fresh solution was made daily. DMSO (10%) was used as a control. Physiologic parameters were recorded according to our previously described method.[25] In brief, a polyethylene catheter was inserted into the femoral artery to sample arterial blood (30 μl) and measure blood pressure. After the catheter had been inserted into the femoral artery, 2 μl of BIX at 2.5 or 10 μg/μl was intracerebroventricularly administered 30 min before the start of the ischemia, because we do not know the permeability of BIX to the blood brain barrier. Body temperature, arterial blood pressure, pO_2, pCO_2, pH, and plasma glucose were measured 15 min after the start of the ischemia. There were no significant differences in physiological parameters between the vehicle- and BIX-treated groups (data not shown). After 30 min of ischemia, vehicle- and BIX-treated mice exhibited moderate neurological deficits (such as circling, decreased resistance to lateral pushing, decreased locomotor activity, flexion of the right (contralateral to the ischemia) torso and forelimb upon lifting the animal by its tail, and abnormal posture). Animals showing no neurological deficits at 30 min after the occlusion were removed from the study on the grounds that they had not undergone successful occlusion of the MCA. We removed 2 out of 15, 1 out of 13, and 1 out of 13 mice in control, 5 μg BIX-treated, and 20 μg BIX-treated groups, respectively. The present experiments were performed in accordance with the Guidelines for Animal Experiments of Gifu Pharmaceutical University.

Neurological deficits. Mice were tested for neurological deficits at 24 h after MCA occlusion and scored as described previously[25] using the following scale: 0 = no observable neurological deficits (normal); 1 = failure to extend the right forepaw (mild); 2 = circling to the contralateral side (moderate); 3 = loss of walking or righting reflex (severe). The investigator who rated the mice was blinded as to the group to which each mouse belonged.

Immunohistochemistry. At 24 h after MCA occlusion, mice were injected with sodium pentobarbital (nembutal; 50 mg/kg, i.p.), and then perfused through the left ventricle with 4% paraformaldehyde in 0.1 M phosphate buffer (PB; pH 7.4). Brains were removed after 15 min of perfusion fixation at 4°C and immersed in the same fixative solution overnight at 4°C. They were then immersed in 25% sucrose in 0.1 M PB for 24 h, and finally frozen in powdered dry ice. Coronal sections (10 μm) were cut on a cryostat at −20°C and stored at −80°C until use. After rehydration, endogenous peroxidase activity was quenched using 1% hydrogen peroxidase in methanol. Next, brain sections were blocked with 3% BSA in PBS/0.1% Triton X-100 for 1 h, and then incubated overnight at 4°C with primary antibody in the same buffer. Sections were washed and then incubated with biotinylated secondary antibody before being incubated for 30 min at room temperature with avidin–biotin–peroxidase complex, and then developed using diaminobenzidine (DAB) peroxidase substrate. Caspase 3-stained cells were counted in the striatum. The results are expressed as positive cells per 1 mm^2.

TUNEL staining. Apoptosis was detected using the TUNEL method using an *in situ* cell death detection kit, POD (Roche, Penzberg, Germany). TUNEL signals were developed using a DAB peroxidase substrate kit (Vector Labs, Burlingame, CA, USA).

***In situ* hybridization histochemistry.** CHOP and GAPDH cDNAs were subcloned into pGEM-T Easy and pBluescript vectors, respectively. Digoxigenin-labeled cRNA probes were made by *in vitro* transcription in the presence of digoxigenin using subcloned cDNAs for these genes as templates. *In situ* hybridization using digoxigenin-labeled cRNA probes was performed as previously described.[27]

Statistical analysis. Statistical comparisons were made using a one-way ANOVA followed by a Student's *t*-test, Dunnett's test, or the Mann–Whitney *U*-test. STATVIEW version 5.0 (SAS Institute Inc., Cary, NC, USA) was used for statistical analyses. $P<0.05$ was considered to indicate statistical significance.

Acknowledgements. We thank Dr. David Ron for the PERK$^{-/-}$ MEFs and the anti-PERK antibody, Dr. Fumihiko Urano for the IRE1$^{-/-}$ MEFs and the anti-IRE1α antibody, Dr. Laurie H Glimcher for the iATF6$\alpha\beta$MEFs, and Dr. K Mori for the BiP-pGL3 reporter plasmid. We also thank Ms Mikiko Kubo for her technical assistance. This work was supported by a Grant-in-Aid for Scientific Research (17200026) from the Japan Society for the Promotion of Science and Research on Psychiatric and Neurological Diseases and Mental Health from the Japan Ministry of Health, Labor, and Welfare. This study was supported by the Program for Promotion of Fundamental Studies in Health Sciences of the National Institute of Biomedical Innovation. Funding was also provided by the Japan Society for the Promotion of Science (SK).

1. Zhang K, Kaufman RJ. The unfolded protein response: a stress signaling pathway critical for health and disease. *Neurology* 2006; **66** (Suppl 1): s102–s109.
2. Katayama T, Imaizumi K, Sato N, Miyoshi K, Kudo T, Hitomi J *et al*. Presenilin-1 mutations downregulate the signalling pathway of the unfolded-protein response. *Nat Cell Biol* 1999; **8**: 479–485.
3. Katayama T, Imaizumi K, Honda A, Yoneda T, Kudo T, Takeda M *et al*. Disturbed activation of endoplasmic reticulum stress transducers by familial Alzheimer's disease-linked presenilin 1 mutations. *J Biol Chem* 2001; **276**: 43446–43454.
4. Yasuda Y, Kudo T, Katayama T, Imaizumi K, Yatera M, Okochi M *et al*. FAD-linked presenilin-1 mutants impede translation regulation under ER stress. *Biochem Biophys Res Commun* 2002; **296**: 313–318.
5. Hitomi J, Katayama T, Eguchi Y, Kudo T, Taniguchi M, Koyama Y *et al*. Involvement of caspase-4 in endoplasmic reticulum stress-induced apoptosis and Aβ-induced cell death. *J Cell Biol* 2004; **165**: 347–356.
6. Kitada T, Asakawa S, Hattori N, Matsumine H, Yamamura Y, Minoshima S *et al*. Mutations in the Parkin gene cause autosomal recessive juvenile Parkinsonism. *Nature* 1998; **392**: 605–608.
7. Imai Y, Soda M, Inoue H, Hattori N, Mizuno Y, Takahashi R. An unfolded putative transmembrane polypeptide, which can lead to endoplasmic reticulum stress, is a substrate of Parkin. *Cell* 2001; **105**: 891–902.
8. Nishitoh H, Matsuzawa A, Tobiume K, Saegusa K, Takeda K, Inoi S *et al*. ASK1 is essential for endoplasmic reticulum stress-induced neuronal cell death triggered by expanded polyglutamine repeats. *Gene Dev* 2002; **16**: 1345–1355.
9. Bence NF, Sampat RM, Kopito RR. Impairment of the ubiquitin–proteasome system by protein aggregation. *Science* 2001; **292**: 1552–1555.
10. Kumar R, Azam S, Sullivan JM, Owen C, Cavener DR, Zhang P *et al*. Brain ischemia and reperfusion activates the eukaryotic initiation factor 2alpha kinase, PERK. *J Neurochem* 2001; **77**: 1418–1421.
11. Paschen W, Aufenberg C, Hotop S, Mengesdorf T. Transient cerebral ischemia activates processing of xbp1 messenger RNA indicative of endoplasmic reticulum stress. *J Cereb Blood Flow Metab* 2003; **23**: 449–461.
12. Boyce M, Bryant KF, Jousse C, Long K, Harding HP, Scheuner D *et al*. A selective inhibitor of eIF2α dephosphorylation protects cells from ER stress. *Science* 2005; **307**: 935–939.
13. Kim AJ, Shi Y, Austin RC, Werstuck GH. Valproate protects cells from ER stress-induced lipid accumulation and apoptosis by inhibiting glycogen synthase kinase-3. *J Cell Sci* 2005; **118**: 89–99.
14. ZaiFang Y, Luo H, Weiming F, Mattson MP. The endoplasmic reticulum stress-responsive protein GRP78 protects neurons against excitotoxicity and apotosis: suppression of oxidative stress and stabilization of calcium homeostasis. *Exp Neurol* 1999; **155**: 302–314.
15. Rao RV, Peel A, Logvinova A, del Rio G, Hermel E, Yokota T *et al*. Coupling endoplasmic reticulum stress to the cell death program: role of the ER chaperone GRP78. *FEBS Lett* 2002; **514**: 122–128.
16. Reddy RK, Mao C, Baumeister P, Austin RC, Kaufman RJ, Lee AS. Endoplasmic reticulum chaperone protein GRP78 protects cells from apoptosis induced by topoisomerase inhibitors: role of ATP binding site in suppression of caspase-7 activation. *J Biol Chem* 2003; **278**: 20915–20924.
17. Gorner C, Ferrario A, Rucker N, Wong S, Lee AS. Glucose regulated protein induction and cellular resistance to oxidative stress mediated by porphyrin photosensitization. *Cancer Res* 1991; **51**: 6574–6579.
18. Li LJ, Li X, Ferrario A, Rucker N, Liu ES, Wong S *et al*. Establishment of a Chinese hamster ovary cell line that expresses grp78 antisense transcripts and suppresses A23187 induction of both GRP78 and GRP94. *J Cell Physiol* 1992; **153**: 575–582.

19. Sugawara S, Takeda K, Lee A, Dennert G. Suppression of stress protein GRP78 induction in tumor B/C10ME eliminates resistance to cell mediated cytotoxicity. *Cancer Res* 1993; **53**: 6001–6005.
20. DeGracia DJ, Montie HL. Cerebral ischemia and the unfolded protein response. *J Neurochem* 2004; **91**: 1–8.
21. Kaufman RJ. Orchestrating the unfolded protein response in health and disease. *J Clin Invest* 2002; **110**: 1389–1398.
22. Tajiri S, Oyadomari S, Yano S, Morioka M, Gotoh T, Hamada JI *et al*. Ischemia-induced neuronal cell death is mediated by the endoplasmic reticulum stress pathway involving CHOP. *Cell Death Differ* 2004; **11**: 403–415.
23. Bertolotti A, Zhang Y, Hendershot LM, Harding HP, Ron D. Dynamic interaction of BiP and ER stress transducers in the unfolded-protein. *Nat Cell Biol* 2000; **2**: 326–332.
24. Chen D, Padiernos E, Ding F, Lossos IS, Lopez CD. Apoptosis-stimulating protein of p53-2 ($ASPP2^{53BP2L}$) is an E2F target gene. *Cell Death Differ* 2005; **12**: 358–368.
25. Hara H, Huang PL, Panahian N, Fishman MC, Moskowitz MA. Reduced brain edema and infarction volume in mice lacking the neuronal isoform of nitric oxide synthase after transient MCA occlusion. *J Cereb Blood Flow Metab* 1996; **16**: 605–611.
26. Hara H, Friedlander RM, Gagliardini V, Ayata C, Fink K, Huang Z *et al*. Inhibition of interleukin 1β converting enzyme family proteases reduces ischemic and excitotoxic neuronal damage. *Proc Natl Acad Sci USA* 1997; **94**: 2007–2012.
27. Honma Y, Kanazawa K, Mori T, Tanno Y, Tojo M, Kiyosawa H *et al*. Identification of a novel gene, OASIS, which encodes for a putative CREB/ATF family transcription factor in the long-term cultured astrocytes and gliotic tissue. *Brain Res Mol Brain Res* 1999; **69**: 93–103.

Effect of an Inducer of BiP, a Molecular Chaperone, on Endoplasmic Reticulum (ER) Stress-Induced Retinal Cell Death

Yuta Inokuchi,[1] Yoshimi Nakajima,[1] Masamitsu Shimazawa,[1] Takanori Kurita,[2] Mikiko Kubo,[3] Atsushi Saito,[4] Hironao Sajiki,[2] Takashi Kudo,[5] Makoto Aihara,[5] Kazunori Imaizumi,[4] Makoto Araie,[5] and Hideaki Hara[1]

Purpose. The effect of a preferential inducer of 78 kDa glucose-regulated protein (GRP78)/immunoglobulin heavy-chain binding protein (BiP; BiP inducer X, BIX) against tunicamycin-induced cell death in RGC-5 (a rat ganglion cell line), and also against tunicamycin- or *N*-methyl-D-aspartate (NMDA)-induced retinal damage in mice was evaluated.

Methods. In vitro, BiP mRNA was measured after BIX treatment using semi-quantitative RT-PCR or real-time PCR. The effect of BIX on tunicamycin (at 2 μg/mL)-induced damage was evaluated by measuring the cell-death rate and CHOP protein expression. In vivo, BiP protein induction was examined by immunostaining. The retinal cell damage induced by tunicamycin (1 μg) or NMDA (40 nmol) was assessed by examining ganglion cell layer (GCL) cell loss, terminal deoxyribonucleotidyl transferase (TdT)-mediated dUTP nick-end labeling (TUNEL) staining, and CHOP protein expression.

Results. In vitro, BIX preferentially induced BiP mRNA expression both time- and concentration-dependently in RGC-5 cells. BIX (1 and 5 μM) significantly reduced tunicamycin-induced cell death, and BIX (5 μM) significantly reduced tunicamycin-induced CHOP protein expression. In vivo, intravitreal injection of BIX (5 nmol) significantly induced BiP protein expression in the mouse retina. Co-administration of BIX (5 nmol) significantly reduced both the retinal cell death and the CHOP protein expression in GCL induced by intravitreal injection of tunicamycin or NMDA.

Conclusions. These findings suggest that this BiP inducer may have the potential to be a therapeutic agent for endoplasmic reticulum (ER) stress–induced retinal diseases. (*Invest Ophthalmol Vis Sci.* 2009;50:334–344) DOI:10.1167/iovs.08-2123

The endoplasmic reticulum (ER) is the cellular organelle in which proteins (destined for secretion or for diverse subcellular localizations) are not only synthesized, but acquire their correct conformation. Perturbations of the environment normally required for protein folding in the ER, or the production of large amounts of misfolded proteins exceeding the functional capacity of the organelle, trigger a pattern of physiological response in the cell, collectively known as the unfolded protein response (UPR).[1–3] The UPR serves to cope with ER stress by transcriptionally regulating ER chaperones and other ER-resident proteins, attenuating the overall translation rate, and increasing the degradation of misfolded ER proteins. ER stress is caused by the accumulation of unfolded proteins in the ER lumen, and it is associated with various neurodegenerative diseases such as Alzheimer's, Huntington's, and Parkinson's diseases, and with type-1 diabetes.[4–6] Recent reports have shown that ER stress is also involved in a variety of experimental retinal neurodegenerative models, such as those of diabetic retinopathy,[7] retinitis pigmentosa,[8,9] and glaucoma.[10,11]

Recently, we reported that BiP expression is upregulated in the retina after intravitreal injection of either tunicamycin or NMDA (a glutamate-receptor agonist).[12,13] Tunicamycin, a glucosamine-containing nucleoside antibiotic, produced by genus *Streptomyces*, is an inhibitor of *N*-linked glycosylation and the formation of *N*-glycosidic protein-carbohydrate linkages.[14] Tunicamycin, which reduces the *N*-glycosylation of proteins, causes an accumulation of unfolded proteins in the ER and thus induces ER stress. Awai et al.[15] previously had demonstrated that NMDA induces CHOP protein (a member of the CCAAT/enhancer-binding protein family induced by ER stress) in GCL and the inner plexiform layer (IPL), and that CHOP$^{-/-}$ mice are more resistant to NMDA-induced retinal cell death than wild-type mice. These findings indicate that ER stress may be involved in these models of retinal injury.

BiP, a highly conserved member of the 70 kDa heat shock protein family, is one of the chaperones localized to the ER membrane,[16,17] and it is a major ER-luminal Ca^{2+}-storage protein.[18,19] BiP works to restore folding in misfolded or incompletely assembled proteins,[20–22] the interaction between BiP and misfolded proteins being dependent on its hydrophobic motifs.[23–25] Proteins stably bound to BiP are subsequently translocated from the ER into the cytosol, where they are degraded by proteasomes.[26,27] Previous reports have show that induction of BiP prevents the neuronal death induced by ER stress.[28–31] Hence, a selective inducer of BiP might attenuate ER stress and be a new, useful therapeutic agent for the treatment of ER stress-associated diseases.

This seemed an interesting idea, and we recently identified BiP inducer X (BIX) while screening for low molecular

From the Departments of [1]Biofunctional Evaluation, Molecular Pharmacology and [2]Medicinal Chemistry, Gifu Pharmaceutical University, Gifu, Japan; [3]Department of Psychiatry, Osaka University Graduate School of Medicine, Osaka, Japan; [4]Division of Molecular and Cellular Biology, Department of Anatomy, Faculty of Medicine, University of Miyazaki, Miyazaki, Japan; and [5]Department of Ophthalmology, University of Tokyo School of Medicine, Tokyo, Japan.

Supported in part by a Grant-in-Aid (No.18209053) for scientific research from the Ministry of Education, Science, Sports, Culture of the Japanese Government; by a research grant (No.18210101) from the Ministry of Health, Labor, and Welfare of the Japanese Government, and by Grant-in-Aid for Japan Society for the Promotion of Science Fellows.

Submitted for publication April 4, 2008; revised July 25, 2008; accepted October 27, 2008.

Disclosure: **Y. Inokuchi**, None; **Y. Nakajima**, None; **M. Shimazawa**, None; **T. Kurita**, None; **M. Kubo**, None; **A. Saito**, None; **H. Sajiki**, None; **T. Kudo**, None; **M. Aihara**, None; **K. Imaizumi**, None; **M. Araie**, None; **H. Hara**, None

The publication costs of this article were defrayed in part by page charge payment. This article must therefore be marked "*advertisement*" in accordance with 18 U.S.C. §1734 solely to indicate this fact.

Corresponding author: Hideaki Hara, Department of Biofunctional Evaluation, Molecular Pharmacology, Gifu Pharmaceutical University, 5-6-1 Mitahora-higashi, Gifu 502-8585, Japan; hidehara@gifu-pu.ac.jp.

Investigative Ophthalmology & Visual Science, January 2009, Vol. 50, No. 1

mass compounds that might induce BiP using high-throughput screening (HTS) with a BiP reporter assay system (Dual-Luciferase Reporter Assay; Promega Corporation, Madison, WI).[32] We found that BIX preferentially induced BiP mRNA and protein in SK-N-SH cells and reduced tunicamycin-induced cell death. Intracerebroventricular pretreatment with BIX reduced the infarction size after focal cerebral ischemia in mice. In view of the retinal research described above, we wondered whether BIX might reduce the retinal ganglion cell loss and CHOP expression induced by tunicamycin or NMDA treatment.

In the present study, we examined primarily whether induction of BiP might inhibit the retinal cell death induced by tunicamycin in RGC-5 cells in vitro, and/or that induced by tunicamycin or NMDA in mice in vivo.

Materials and Methods

All experiments were performed in accordance with the ARVO Statement for the Use of Animals in Ophthalmic and Vision Research, and they were approved and monitored by the Institutional Animal Care and Use Committee of Gifu Pharmaceutical University, Gifu, Japan.

Materials

Dulbecco modified Eagle medium (DMEM) and NMDA were purchased from Sigma-Aldrich (St. Louis, MO). The other drugs used and their sources were as follows: BIX, 1-(3,4-dihydroxyphenyl)-2-thiocyanatoethanone, was synthesized in the Department of Medicinal Chemistry, Gifu Pharmaceutical University, while tunicamycin was purchased from Wako (Osaka, Japan). Isoflurane was acquired from Nissan Kagaku (Tokyo, Japan) and fetal bovine serum (FBS) was from Valeant (Costa Mesa, CA).

RGC-5 Culture

RGC-5[32] were gifted by Neeraj Agarwal (Department of Pathology and Anatomy, UNT Health Science Center, Fort Worth, TX). Cultures of RGC-5 were maintained in DMEM supplemented with 10% FBS, 100 U/mL penicillin (Meiji Seika Kaisha Ltd., Tokyo, Japan), and 100 μg/mL streptomycin (Meiji Seika Kaisha, Ltd.) in a humidified atmosphere of 95% air and 5% CO_2 at 37°C. The RGC-5 cells were passaged by trypsinization every 3 days, as in our previous reports.[12,13,33] We used RGC-5 without any differentiation.

RNA Isolation and Semi-Quantitative RT-PCR Analysis

To examine the effect of BIX on BiP mRNA expression, RGC-5 cells were seeded in six-well plates at a density of 1.4×10^5 cells per well. After the cells had been incubating for 24 h, they were exposed to 50 μM BIX in 1% FBS DMEM for 0.5, 1, 2, 4, 6, 8, or 12 h, or to 2, 10, 50, or 150 μM BIX in 1% FBS DMEM for 6 h. Total RNA was extracted (RNeasy Mini Kit; QIAGEN KK, Tokyo, Japan) according to the manufacture's protocol. The total RNA was divided into microtubes, and frozen to −80°C. RNA concentrations were determined spectrophotometrically at 260 nm. First-strand cDNA was synthesized in a 20-μl reaction volume using a random primer (Takara, Shiga, Japan) and Moloney murine leukemia virus reverse transcriptase (Invitrogen, Carlsbad, CA). PCR was performed in a total volume of 30 μL containing 0.8 μM of each primer, 0.2 mM dNTPs, 3 U *Taq* DNA polymerase (Promega), 2.5 mM $MgCl_2$, and 1× PCR buffer. The amplification conditions for the semi-quantitative RT-PCR analysis were as follows: an initial denaturation step (95°C for 5 minutes), 20 cycles of 95°C for 1 minute, 55°C for 1 minute, and 72°C for 1 minute, and a final extension step (72°C for 7 minutes). The numbers of amplification cycles for the detection of BiP and β-actin were 18 and 15, respectively. The primers used for amplification were as follows: BiP: 5′-GTTTGCTGAGGAAGACAAAAAGCTG-3′ and 5′-CACTTCCATAGAGTTTGCTGATAATTG-3′; β-actin: 5′-TCCTCCCTGGAGAAGAGCTAC-3′ and 5′-TCCTGCTTGCTGATCCACAT-3′.

PCR products were resolved by electrophoresis through 6% (w/v) polyacrylamide gels. The density of each band was quantified using an imaging program (Scion Image Program; Scion Corporation, Frederick, MD).

Real-Time PCR

Real-time PCR (TaqMan; Applied Biosystems, Foster City, CA) was performed as described previously.[34] Single-stranded cDNA was synthesized from total RNA using a high-capacity cDNA archive kit (Applied Biosystems). Quantitative real-time PCR was performed using a sequence detection system (ABI PRISM 7900HT; Applied Biosystems) with a PCR master mix (TaqMan Universal PCR Master Mix; Applied Biosystems), according to the manufacturer's protocol. mRNA expression was measured by real-time PCR using a gene expression product (Assays-on-Demand Gene Expression Product; Applied Biosystems) and a BiP probe (Assay ID Details: Mm00517691). The thermal cycler conditions were as follows: 2 minutes at 50°C and then 10 minutes at 95°C, followed by two-step PCR for 50 cycles consisting of 95°C for 15 seconds followed by 60°C for 1 minute. For each PCR, we obtained the slope value, R^2 value, and linear range of a standard curve of serial dilutions. All reactions were performed in duplicate. The results are expressed relative to the β-actin (Assay ID Details: Mm00661904) internal control.

Cell Viability

To examine the effects of BIX on the cell death induced by tunicamycin (2 μg/mL) or staurosporine (an ER stress-independent apoptosis inducer, 30 nM) RGC-5 cells were seeded at a low density of 700 cells per well into 96-well plates. After pretreatment with BIX for 12 h, tunicamycin or staurosporine was added to the cultures for 48 h or 24 h, respectively. Cell death was assessed on the basis of combination staining with the fluorescent dyes Hoechst 33342 and propidium iodide (PI; Molecular Probes, Eugene, OR) or the change in fluorescence intensity after the cellular reduction of WST-8 to formazan. Hoechst 33342 (λex 350 nm, λem 461 nm) and PI (λex 535 nm, λem 617 nm) were added to the culture medium at final concentrations of 8 and 1.5 μM, respectively, for 30 minutes. Images were collected using a CCD camera (DP30VW; Olympus America, Center Valley, PA) via an epifluorescence microscope (IX70; Olympus, Tokyo, Japan) fitted with fluorescence filters for Hoechst 33342 (U-MWU; Olympus), and PI (U-MWIG; Olympus). In WST-8 assay, cell viability was assessed by culturing cells in a culture medium containing 10% WST-8 (Cell Counting Kit-8; Dojin Kagaku, Kumamoto, Japan) for 3 h at 37°C, with quantification being achieved by scanning with a microplate reader at 492 nm.[35] This absorbance is expressed as a percentage of that in control cells (which were in 1% FBS DMEM) after subtraction of background absorbance.

Animals

Mice used were male adult ddY mice (Japan SLC, Hamamatsu, Japan), male adult Thy-1-cyan fluorescent protein (CFP) transgenic mice (The Jackson Laboratory, Bar Harbor, Maine),[36] and ER stress-activated indicator (ERAI)-transgenic mice carrying the F-XBP1ΔDBD-venus, a variant of green fluorescent protein (GFP) fusion gene, which allows effective identification of cells under ER stress in vivo, as previously described by Iwawaki et al.[37] Briefly, when ER stress in ERAI transgenic mice was induced, splicing of mRNA encoding the XBP-1 fusion gene occurs and the spliced form of F-XBP1ΔDBD-venus fusion gene could be translated into fluorescent protein. Thus, it is visualized by the fluorescence intensity arising from the XBP-Δ-venus fusion protein during ER stress, and we measured it by fluorescence microscopy and immunoblotting in the present study.

All mice were kept under controlled lighting conditions (12 h:12 h light/dark). The mouse genotype was determined by applying standard PCR methodology to tail DNA.

NMDA- or Tunicamycin-Induced Retinal Damage

NMDA- or tunicamycin-induced retinal damage was produced as previously reported by Siliprandi et al. (1992).[38] Briefly, mice were anesthetized with 3.0% isoflurane and maintained with 1.5% isoflurane in 70% N_2O and 30% O_2 via an animal general anesthesia machine (Soft Lander; Sin-ei Industry Co. Ltd., Saitama, Japan). The body temperature was maintained between 37.0 and 37.5°C with the aid of a heating pad. Retinal damage was induced by the injection (2 μL/eye) of NMDA (Sigma-Aldrich) at 20 mM or tunicamycin at 1 μg/mL dissolved in 0.01 M PBS with 5% dimethyl sulfoxide (DMSO). Each solution was injected into the vitreous body of the left eye under the above anesthesia. One drop of 0.01% levofloxacin ophthalmic solution (Santen Pharmaceuticals Co. Ltd., Osaka, Japan) was applied topically to the treated eye immediately after the intravitreal injection. Seven days after the injection, eyeballs were enucleated for histologic analysis. For comparative purposes, nontreated retinas from each mouse strain were also investigated. BIX (0.5 or 5 nmol) or vehicle (5% DMSO in PBS) was co-administered with the NMDA or tunicamycin in each mouse.

Histologic Analysis

In mice under anesthesia produced by an intraperitoneal injection of sodium pentobarbital (80 mg/kg), each eye was enucleated and kept immersed for at least 24 h at 4°C in a fixative solution containing 4% paraformaldehyde. Six paraffin-embedded sections (thickness, 4 μm) cut through the optic disc of each eye were prepared in a standard manner and stained with hematoxylin and eosin. The damage induced by NMDA or tunicamycin was then evaluated, with three sections from each eye being used for the morphometric analysis, as described below. Light-microscope images were photographed, and the cells in the GCL at a distance between 375 and 625 μm from the optic disc were counted on the photographs in a masked fashion by a single observer (Y.I.). Data from three sections (selected randomly from the six sections) were averaged for each eye and used to evaluate the cell count in the GCL.

Retinal Flatmounts and Analysis in Transgenic Mice

Transgenic mice were given an overdose of sodium pentobarbital, and retinas were dissected out and fixed for 30 minutes in 4% paraformaldehyde diluted in 0.1 M phosphate buffer (PB) at pH 7.4. Retinas were subsequently washed with PBS at room temperature, flatmounted on clean glass slides using fluorescent mounting medium (Dako Corp., Carpinteria, CA), and stored in the dark at 4°C for 1 week. The damage induced by tunicamycin was then evaluated, with four sections (dorsal, ventral, temporal, and nasal) from each eye being used for the morphometric analysis, as described below. At various times after intravitreal injections (24 h in ERAI mice and 7 days in Thy-1-CFP transgenic mice), fluorescent images were photographed (×200, 0.144 mm^2) using an epifluorescence microscope (BX50; Olympus) fitted with a CCD camera (DP30VW; Olympus). In the case of Thy-1-CFP transgenic mice, Thy-1-CFP-positive cells at a distance of 1 mm from the optic disc were counted on the photographs in a masked fashion by a single observer (Y.I.). Data from the four parts of each eye were used to evaluate the RGC count.[39]

Immunostaining

Eyes were enucleated as described under Histologic Analysis, fixed in 4% paraformaldehyde overnight at 4°C, immersed in 25% sucrose for 48 h at 4°C, and embedded in optimum cutting temperature (OCT) compound (Sakura Finetechnical Co. Ltd, Tokyo, Japan). Transverse 10-μm thick cryostat sections were cut and placed onto slides (MAS COAT; Matsunami Glass Ind., Ltd., Osaka, Japan). Immunohistochemical staining was performed according to the following protocol: Briefly, tissue sections were washed in 0.01 M PBS for 10 minutes, and then endogenous peroxidase was quenched by treating the sections with 3% hydrogen peroxide in absolute methanol for 10 minutes, followed by a pre-incubation with 10% normal goat serum. They were then incubated overnight at 4°C with the following primary antibodies: against CHOP (1:1000 dilution in PBS; Santa Cruz, CA), and against BiP/GRP78 (1:1000 dilution in PBS; BD Transduction Laboratories, Lexington, KY). Sections were washed and then incubated with biotinylated anti-rabbit IgG or anti-mouse IgG. They were subsequently incubated with the avidin-biotin-peroxidase complex for 30 minutes, and then developed using diaminobenzidine (DAB) peroxidase substrate. Images were obtained using a digital camera (COOLPIX 4500; Nikon, Tokyo, Japan).

Quantitation of Density

In the DAB-labeled areas of anti-BiP/GRP78 (BD Transduction Laboratories) and anti-CHOP (Santa Cruz) in the GCL and IPL at a distance between 475 and 525 μm (50 × 50 μm) from the optic disc, retinal DAB-labeled cell density was evaluated by means of appropriately calibrated computerized image analysis, using median density in the range of 0 to 255 as an analysis tool (Image Processing and Analysis in Java, Image J; National Institute of Mental Health, Bethesda, MD) and averaged for two areas.[40] The data lie within the dynamic range of this assays

Briefly, light-microscope images of the above-mentioned areas were photographed, inverted in a gradation sequence using image editing software (Adobe Photoshop 5.5; Adobe Systems Inc., San Jose, CA), and then optical intensity was evaluated using Image J. The score for the negative-control (nontreated with first antibody), as the background value, was subtracted from the scores.

TUNEL Staining

TUNEL staining was performed according to the manufacturer's protocol (In Situ Cell Death Detection Kit; Roche Biochemicals, Mannheim, Germany) to detect the retinal cell death induced by NMDA. Mice were anesthetized with pentobarbital sodium at 80 mg/kg, IP, 24 h after intravitreal injection (either of NMDA 40 nmol/eye or of tunicamycin 1 μg/eye). The eyes were enucleated, fixed overnight in 4% paraformaldehyde, and immersed for 2 days in 25% sucrose with PBS. The eyes were then embedded in a supporting medium (OCT compound) for frozen-tissue specimens. Retinal sections at 10-μm thick were cut on a cryostat at −25°C, and stored at −80°C until staining. After twice washing with PBS, sections were incubated with terminal TdT enzyme at 37°C for 1 h, then washed 3 times in PBS for 1 minute at room temperature. Sections were subsequently incubated with an anti-fluorescein antibody-peroxidase conjugate at room temperature in a humidified chamber for 30 minutes, then developed using DAB tetrahydrochloride peroxidase substrate. Light-microscope images were photographed, and the labeled cells in the GCL at a distance between 375 and 625 μm from the optic disc were counted in two areas of the retina in a masked fashion by a single observer (Y.I.). The number of TUNEL-positive cells was averaged for these two areas, and plotted as the number of TUNEL-positive cells.

Western Blot Analysis

RGC-5 cells were lysed using a cell-lysis buffer (RIPA buffer R0278; Sigma-Aldrich) with protease (P8340; Sigma-Aldrich) and phosphatase inhibitor cocktails (P2850 and P5726; Sigma-Aldrich), and 1 mM EDTA. In vivo, mice were euthanatized using sodium pentobarbital at 80 mg/kg, IP, and their eyeballs were quickly removed. The retinas were carefully separated from the eyeballs and quickly frozen in dry ice. For protein extraction, the tissue was homogenized in the cell-lysis buffer using a homogenizer (Physcotron; Microtec Co. Ltd., Chiba, Japan). The lysate was centrifuged at 12,000*g* for 20 minutes, and the supernatant was used for this study. Assays to determine the protein concentration were performed by comparison with a known concentration of bovine serum albumin using a BCA protein assay kit (Pierce Biotechnology, Rockford, IL). A mixture of equal parts of an aliquot of

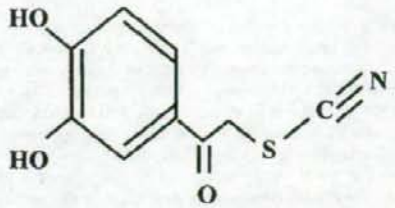

FIGURE 1. The structure of BIX (1-(3,4-dihydroxyphenyl)-2-thiocyanate-ethanone).

protein and sample buffer with 10% 2-mercaptoethanol was subjected to 10% sodium dodecyl sulfate-polyacrylamide gel electrophoresis. The separated protein was then transferred onto a polyvinylidene difluoride membrane (Immobilon-P; Millipore Corporation, Bedford, MA). For immunoblotting, the following primary antibodies were used: rabbit anti-CHOP polyclonal antibody (1:1000; Santa Cruz), mouse anti-β-actin monoclonal antibody (1:4000; Sigma-Aldrich), and rabbit anti-green fluorescent protein (GFP) polyclonal antibody (1:1000; Medical & Biological Laboratories Co. Ltd., Nagoya, Japan). The secondary antibody used was either goat anti-rabbit HRP-conjugated (1:2000) or goat anti-mouse HRP-conjugated (1:2000). The immunoreactive bands were visualized using a chemiluminescent substrate (SuperSignal West Femto Maximum Sensitivity Substrate; Pierce Biotechnology). The band intensity was measured using an imaging analyzer (Lumino Imaging Analyzer; Toyobo, Osaka, Japan) and a gel analysis electrophoresis analysis software (Gel Pro Analyzer; Media Cybernetics, Atlanta, GA).

Statistical Analysis

Data are presented as the means ± SE. Statistical comparisons were made by way of Dunnett's test or Student's *t*-test using statistical analysis software (STAT VIEW version 5.0; SAS Institute, Cary, NC). $P < 0.05$ was considered to indicate statistical significance.

RESULTS

BiP mRNA in RGC-5 Preferentially Induced by BIX

To clarify whether BIX (Fig. 1) induces BiP in RGC-5, we used semi-quantitative RT-PCR and real-time PCR, using a specific primer and a TaqMan probe recognizing BiP mRNA, respectively. Real-time PCR revealed that the level of BiP mRNA was significantly elevated at 0.5 to 12 h (peak at approximately 6 h) after treatment with 50 μM BIX (Fig. 2A). At 6 h after treatment with BIX (2 to 150 μM), BiP mRNA was increased concentration-dependently (Fig. 2B). Next, we used real-time *PCR* to investigate whether BIX might affect the expressions of any other genes related to the ER stress response, such as GRP94, calreticulin, protein kinase inhibitor of 58 kDa ($p58^{IPK}$), or asparagine synthetase (ASNS; Fig. 2C). Real-time PCR revealed significant inductions of ASNS and calreticulin mRNAs at 6 h after treatment with BIX at 2 and 10 μM, respectively. At 50 μM, BIX induced the mRNAs for GRP94 at 12 h, calreticulin at 6 and 12 h, $p58^{IPK}$ at 6 h, and ASNS at 12 h. In contrast, GRP94 mRNA was significantly reduced at 4 h after treatment with 50 μM BIX.

Protective Effect of BIX against ER Stress–Induced Cell Death in RGC-5 Cells

To investigate whether BIX can prevent the cell death induced by ER stress, RGC-5 cells were pretreated for 12 h with or without BIX, then treated with 2 μg/mL tunicamycin, and finally incubated for a further 48 h. Fluorescence micrographs of Hoechst 33342 and PI staining revealed 38.4 ± 4.5% cell death ($n = 8$) at 48 h after tunicamycin treatment, (control: 0.9 ± 0.2%, $n = 8$), and pretreatment with BIX at 1 and 5 μM significantly reduced this cell death (Figs. 3A, 3B). Next, we evaluated the expression of CHOP protein after tunicamycin treatment. There was no CHOP protein expression in either nontreated or BIX-treated cells (Figs. 3C, 3D). On the other

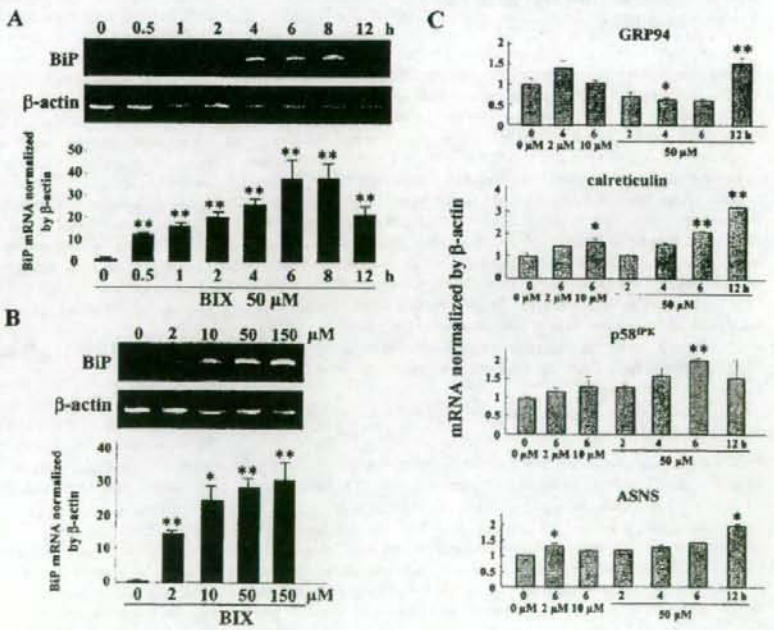

FIGURE 2. Effect of BIX on BiP mRNA expression BIX in RGC-5 cells. (A) Time-dependent induction of BiP mRNA after treatment with 50 μM BIX and (B) concentration-dependence of BIX-induced BiP mRNA expression are each shown by semi-quantitative RT-PCR (*upper panel*) and real-time PCR (*lower panel*). β-Actin mRNA is shown as an internal control. (C) Induction of GRP94, calreticulin, $p58^{IPK}$, and ASNS mRNAs at 6 h after treatment with 2 or 10 μM BIX and at 2 to 12 h after treatment with 50 μM BIX. Data are shown as mean ± SE ($n = 3$ or 4). $^*P < 0.05$, $^{**}P < 0.01$ versus 0 μM (A and B) or 0 μM/0 h (C).

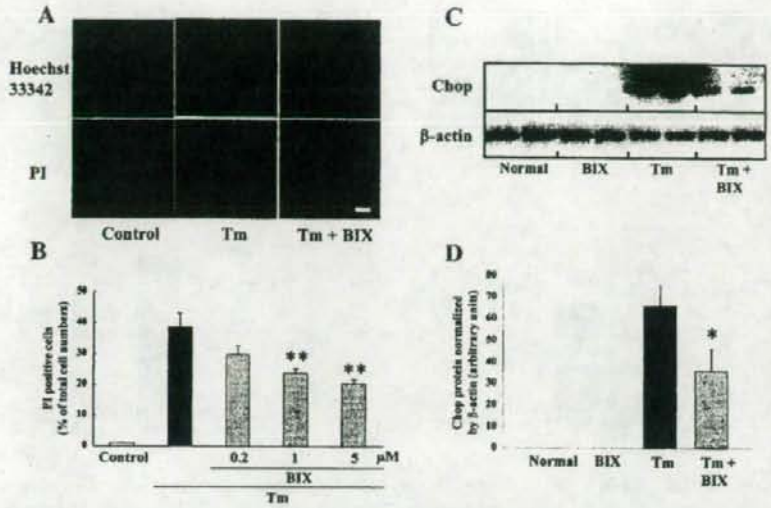

FIGURE 3. Effects of BIX on tunicamycin-induced cell death and CHOP protein expression in RGC-5 cells. (A) RGC-5 cells were pretreated with vehicle or with 1 μM BIX for 12 h, and then immersed in fresh medium (control) or in medium supplemented with 2 μg/mL tunicamycin (Tm; labeled Tm or Tm + BIX). *Upper* photomicrographs show Hoechst 33342 and *lower* ones propidium iodide (PI) staining at 48 h after tunicamycin stimulation. Scale bar represents 25 μm. (B) Numbers of PI-positive cells after tunicamycin treatment. Pretreatment of cells with BIX (1 and 5 μM) significantly reduced the amount of cell death (vs. cells treated with tunicamycin alone). (C) Immunoblot of CHOP protein shows that tunicamycin induced significant CHOP expression, and that pretreatment of cells with BIX at 5 μM reduced this expression with no change in the level of β-actin. *Upper panel* shows CHOP and *lower panel* shows β-actin. (D) Quantitative representations of β-actin-based tunicamycin-induced CHOP protein expression (in arbitrary units). Data are shown as mean ± SE (n = 6 or 8). $^*P < 0.05$, $^{**}P < 0.01$ versus tunicamycin alone.

hand, tunicamycin markedly induced CHOP protein, while pretreatment with BIX at 5 μM reduced this expression to almost half the value seen after tunicamycin treatment alone (Figs. 3C, 3D).

Effects of BIX on Cell Damage Induced by Staurosporine in RGC-5 Culture

To investigate whether BIX protects non-ER stress-induced cell death, we examined staurosporine-induced cell death. Staurosporine at 30 nM for 24 h reduced cell viability to approximately 60% of control (Fig. 4). There was no statistical difference between BIX (1 and 5 μM)-treated and vehicle-treated group.

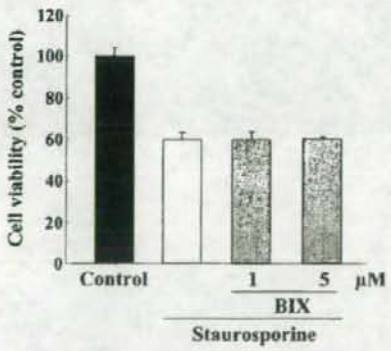

FIGURE 4. Effect of BIX on the cell death induced by staurosporine in RGC-5. RGC-5 cells were pretreated with vehicle or with BIX (1 or 5 μM) for 12 h, and then immersed in fresh medium (control) or in medium supplemented with staurosporine at 30 nM. At the end of this culture period, cell death was assessed by WST-8 assay (Cell Counting Kit-8; Dojin Kagaku). Data are shown as mean ± SE (n = 6).

BiP Protein in the Mouse Retina Induced by Intravitreous Injection of BIX

Compared with that in the nontreated retina, BiP protein expression in GCL and IPL was significantly increased at 6 and 12 h after intravitreal injection of BIX (5 nmol; Figs. 5A, 5B). Optical density analysis confirmed that administration of BIX induced BiP protein in vivo (Fig. 5D).

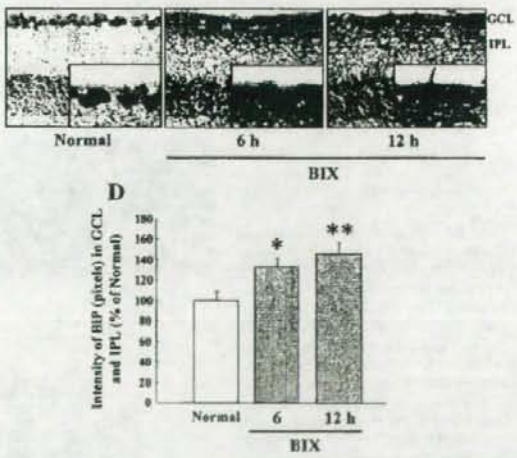

FIGURE 5. BiP protein expression in the mouse retina induced by intravitreous injection of BIX. Immunostaining probed with an antibody against BiP/GRP78. (A) Nontreated, (B) 6 h, and (C) 12 h after intravitreous injection of BIX (5 nmol). (D) Expression ratio for BiP induction intravitreous injection of BIX is represented as the ratio of intensity values. Data are shown as mean ± SE (n = 6). $^*P < 0.05$, $^{**}P < 0.01$ versus nontreated normal retina. Each scale bar represents 25 μm.

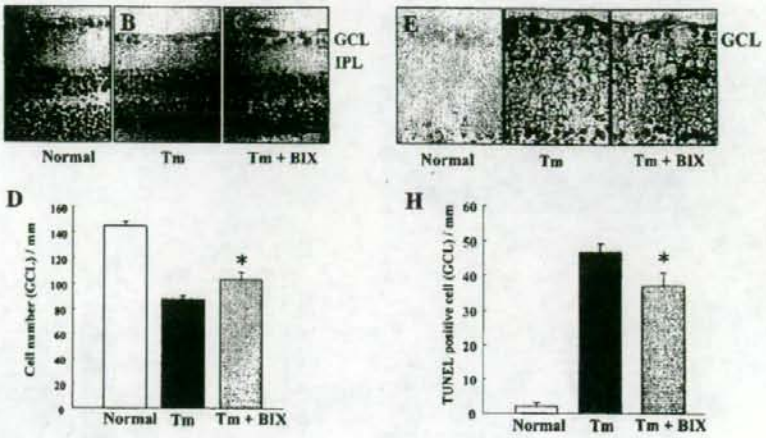

FIGURE 6. Effects of BIX on retinal damage induced by intravitreal injection of tunicamycin in mice. Hematoxylin and eosin staining of cross-sections of (A) nontreated, (B) Tm-treated, and (C) Tm plus BIX-treated mouse retinas at seven days after intravitreal injection of tunicamycin (1 μg) either alone or with BIX (5 nmol). (D) Damage was evaluated by counting cell numbers in GCL at seven days after the above injections. TUNEL staining of cross-sections of (E) nontreated, (F) Tm-treated, and (G) Tm plus BIX-treated mouse retinas at seven days after the above injections. (H) Effect of BIX on Tm-induced expression of TUNEL-positive cells at 24 h after the above injections. Data are shown as mean ± SE ($n = 9$ or 10). *$P < 0.05$ versus tunicamycin alone. Scale bars each represent 25 μm.

Protective Effect of BIX against Tunicamycin-Induced Retinal Damage in Mice

Tunicamycin decreased the cell number in GCL at 7 days after its intravitreal injection (vs. nontreated retinas; Figs. 6A, 6B). There was significantly less cell loss in GCL when BIX (5 nmol) was co-administered with the tunicamycin (Figs. 6B–6D). In addition, intravitreal injection of tunicamycin increased the number of TUNEL-positive cells in GCL at 24 h (vs. nontreated retinas; Figs. 6E, 6F). BIX (5 nmol), when co-administered with the tunicamycin, significantly reduced the number of TUNEL-positive cells (vs. tunicamycin alone; Figs. 6F–6H).

Protective Effect of BIX against Tunicamycin-Induced Retinal Damage in Thy-1-CFP Transgenic Mice

In this experiment on Thy-1-CFP transgenic mice, we confirmed the effect of BIX in a larger retinal area than that evaluated in Figure 6D. We counted the number of Thy-1-CFP-positive cells (in flatmounts) in the four white areas shown 1 mm from the center of the optic disc in Figure 7E, and then totaled these values. In the Thy-1-CFP-transgenic mouse retina, axonal fibers were evenly and densely distributed. There were congested CFP-positive cells in the vehicle-treated retina (Fig. 7A), and no change was observed in BIX-treated retinas without tunicamycin treatment (Fig. 7B). Intravitreal injection of tunicamycin decreased the Thy-1-CFP-positive cell count at 7 days (vs. vehicle-treated retina; Figs. 7A, 7C). BIX at 5 nmol, when co-administered with the tunicamycin, significantly inhibited this cell loss (Figs. 7C, 7D, 7F).

Effect of BIX on Tunicamycin-Induced CHOP Expression in Mice

Representative photograph of a nontreated retina is shown in Figure 8A. No change was observed in the BIX-treated retina (Fig. 8B). Optical density analysis of CHOP protein immunoreactivity in GCL and IPL showed that intravitreal injection of tunicamycin (1 μg) significantly increased the level of CHOP protein at 72 h after the injection (Fig. 8C). BIX (5 nmol), when co-administered with the tunicamycin, significantly inhibited this effect (Figs. 8D, 8E).

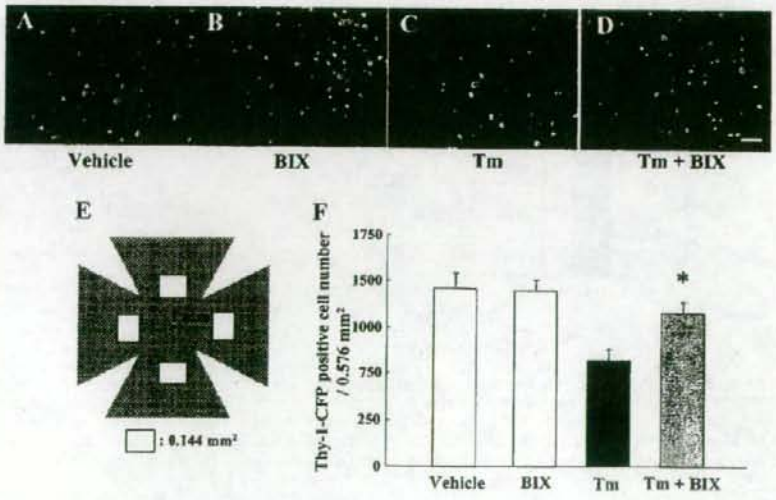

FIGURE 7. Effects of BIX on retinal damage induced by intravitreal injection of tunicamycin in Thy-1-CFP transgenic mice. Mouse retinas (flatmounts) at seven days after intravitreal injection of (A) vehicle, (B) BIX (5 nmol), (C) Tm (1 μg), or (D) Tm (1 μg) plus BIX (5 nmol). Damage was evaluated by counting Thy-1-CFP-positive cell numbers in the four *white* areas shown in (E) (each area 0.144 mm² × 4 areas; total 0.576 mm²) at seven days after the above intravitreal injections. (F) Effect of BIX against Tm-induced damage (indicated by decreased number of Thy-1-CFP-positive cells) at seven days after intravitreal injection. Data are shown as mean ± SE ($n = 9$ or 10). *$P < 0.05$ versus tunicamycin alone. Scale bar represents 25 μm.

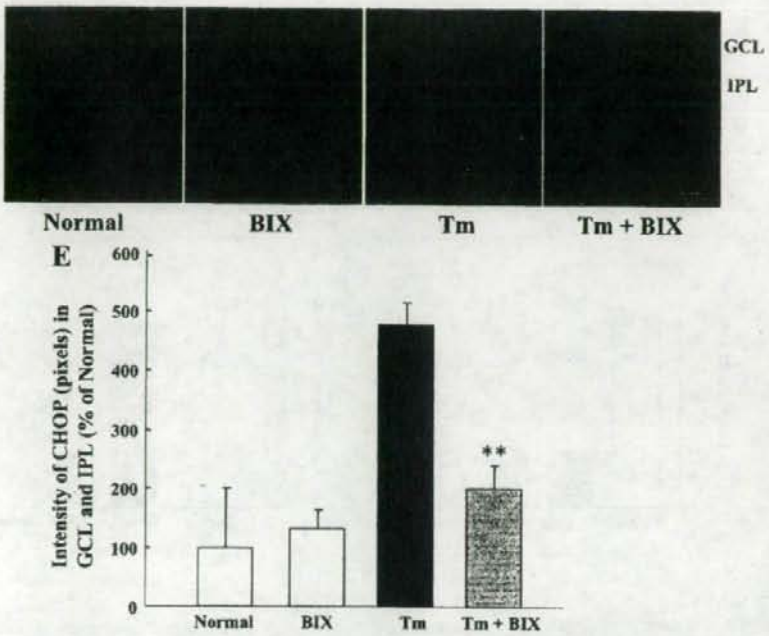

FIGURE 8. Effect of BIX on tunicamycin-induced CHOP expression in the mouse retina. Mouse retinas (cross-sections) either (A) nontreated or at three days after intravitreal injection of (B) BIX (5 nmol), (C) Tm (1 μg) or (D) Tm (1 μg) plus BIX (5 nmol). (E) Relative density of CHOP protein expression in GCL and IPL at three days after the above intravitreal injections. Data are shown as mean ± SE ($n = 6$). $^{**}P < 0.01$ versus tunicamycin alone. Scale bar represents 25 μm.

Effect of BIX on Tunicamycin-Induced XBP-1 Expression in ERAI Mice

In ERAI mice, the fluorescence intensity arising from the XBP-1-venus fusion protein (indicating ER stress activation) can be easily visualized, allowing evaluation of the effect of ER stress on the retina. In the representative photographs of flatmount retinas from ERAI mice shown in Figure 9, no difference was observed between vehicle-treated and BIX-treated retinas (Fig. 9B). Intravitreal injection of tunicamycin (1 μg) induced XBP-1-venus expression (vs. the vehicle-treated retina; Fig. 9C). Immunoblot analysis of XBP-1-venus protein expression in the retina (using an anti-GFP antibody) showed that intravitreal injection of tunicamycin (1 μg) significantly raised the level of XBP-1-venus protein, and that BIX (5 nmol), when co-administered with the tunicamycin (Fig. 9D), significantly inhibited this effect (Figs. 9E, 9F).

Protective Effect of BIX against NMDA-Induced Retinal Damage in Mice

A representative photograph of a nontreated retina is shown in Figure 10A. Intravitreal injection of NMDA (a) decreased the

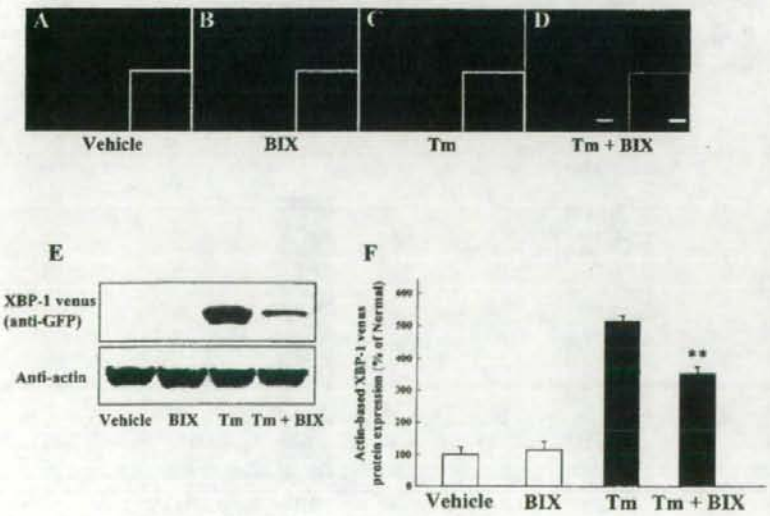

FIGURE 9. Effect of BIX on tunicamycin-induced XBP-1 venus expression in ERAI mice. Mouse retinas (flatmounts) at 24 h after intravitreal injection of (A) vehicle, (B) BIX (5 nmol), (C) Tm (1 μg) or (D) Tm (1 μg) plus BIX (5 nmol). (E) *Upper panel* shows XBP-1 venus protein expression, while *lower panel* shows β-actin protein expression at 24 h after the above injections. (F) Western blot analysis showing effect of BIX on Tm-induced expression of β-actin-based XBP-1 venus protein expression at 24 h after the above injections. Data are shown as mean ± SE ($n = 8$). $^{*}P < 0.01$ versus tunicamycin alone. Scale bars in main photomicrographs and in *insets* represent 25 and 5 μm, respectively.

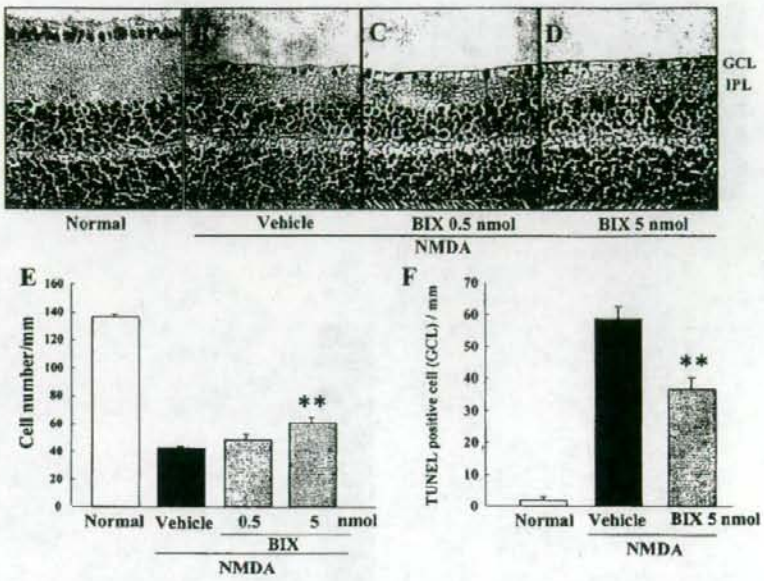

FIGURE 10. Effects of BIX on retinal damage induced by intravitreal injection of NMDA in mice. Mouse retinas (cross-sections) either (A) nontreated or at seven days after intravitreal injection of (B) NMDA (40 nmol) alone or (C, D) NMDA (40 nmol) plus BIX (0.5 or 5 nmol). (E) Damage was evaluated by counting cell numbers in GCL at seven days after the above intravitreal injections. (F) Effect of BIX on NMDA-induced expression of TUNEL-positive cells at 24 h after intravitreal injection of NMDA (40 nmol) either alone or with BIX (5 nmol). Data are shown as mean ± SE ($n = 9$ or 10). $^{**}P < 0.01$ versus NMDA-treated control group. Scale bar represents 25 μm.

cell number in GCL at 7 days (Figs. 10B, 10E) and (b) increased the number of TUNEL-positive cells in GCL at 24 h (vs. nontreated normal retina; Fig. 10F). BIX (5 nmol), when co-administered with the NMDA, significantly reduced (vs. NMDA alone) both the cell loss in GCL (Figs. 10D, 10E) and the number of TUNEL-positive cells (Fig. 10F). On the other hand, there was no statistical difference between BIX (0.5 nmol)- and vehicle-treated group in NMDA-induced cell death in GCL (Figs. 10C, 10E).

Effect of BIX on NMDA-Induced CHOP Expression in Mice

A representative photograph of a nontreated retina is shown in Figure 11A and no change was detected between nontreated

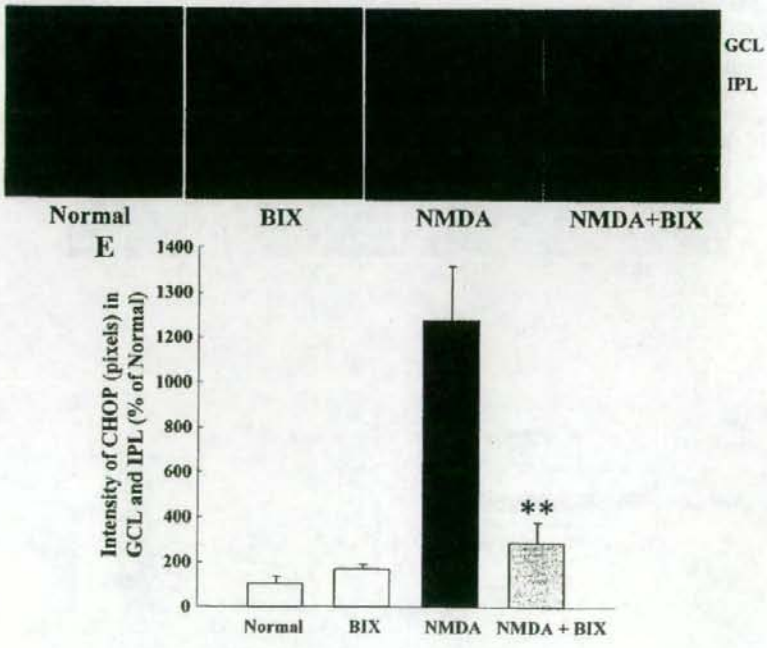

FIGURE 11. Effect of BIX on NMDA-induced CHOP expression in mice. Mouse retinas (cross-sections) either (A) nontreated or at three days after intravitreal injection of (B) NMDA (40 nmol) alone or (C) NMDA (40 nmol), or (D) NMDA (40 nmol) plus BIX (5 nmol). (E) Relative density of CHOP protein expression in GCL and IPL at three days after the above intravitreal injections. Data are shown as mean ± SE ($n = 6$). $^{**}P < 0.01$ versus NMDA alone. Scale bar represents 25 μm.

retina and the BIX-treated retina without NMDA treatment (Figs. 11A, 11B). Optical density analysis of CHOP protein immunoreactivity in GCL and IPL showed that intravitreal injection of NMDA (40 nmol) significantly increased the level of CHOP protein at 72 h after the injection (Fig. 11C). When co-administered with the NMDA, BIX (5 nmol) significantly inhibited this effect (Figs. 11D, 11E).

Discussion

In the present study, we confirmed that BIX preferentially induces BiP mRNA in RGC-5. Although it also induced GRP94, calreticulin, p58^{IPK}, and ASNS, these inductions were lower than that of BiP. This is consistent with our previous study that BIX preferentially induced BiP with slight inductions of GRP94, calreticulin, and CHOP mediated by the activating transcription factor 6 (ATF6) pathway accompanied by activation of ERSEs, and that BIX does not affect the pathway downstream of IRE1 or the translational control branch downstream of PERK in SK-N-SH cells.[32] Therefore, BIX is not just an ER stressor such as tunicamycin or thapsigargin, and we consider that the induction of BiP by BIX is mediated by the ATF6 pathway in RGC-5 similar to that in SK-N-SH cells. Next, we evaluated the effects of BIX, as a preferential inducer of BiP, on ER stress–induced in vitro cell death in RGC-5 (a rat ganglion cell-line) and in vivo retinal damage in mice. We found that BIX reduced tunicamycin-induced cell death in RGC-5 and also reduced both tunicamycin-induced and NMDA-induced retinal damage in mice. Our previous study revealed that BIX (a) reduced tunicamycin-induced cell death in SK-N-SH cells, (b) contributed to the induction of BiP expression via the ATF-6 pathway (but not via the PERK or IRE1 pathways), and (c) on intracerebroventricular injection, prevented the neuronal damage induced by focal ischemia in mice.[32] Furthermore, immunostaining revealed that intravitreal injection of BIX significantly induced BiP protein in mouse retina. Particularly, it expressed in GCL and IPL (versus both the normal and the sham retina). On the other hand, there was little protective effect of BIX against RGC-5 damages after staurosporine treatment. Staurosporine is well known as a nonspecific inhibitor of protein kinases and initiates caspase-dependent apoptosis in many cell types.[41,42] Our previous studies revealed that staurosporine induced cell death without any changes in the expression of BiP or CHOP protein.[12,43] Furthermore, preliminary study showed that treatment with BIX (1 and 5 μM) did not inhibit RGC-5 cell death 48 h after serum deprivation, which does not induce any UPR-responses such as BiP or CHOP (unpublished data). These results strongly support that BIX selectively protects cell damage induced by ER stress.

Recently, we reported that in mice, increased expressions of XBP-1 splicing, BiP, and CHOP could be detected after the induction of retinal damage by tunicamycin, NMDA, or an elevation of intraocular pressure.[13] That report was the first to demonstrate an involvement of ER stress and BiP in retinal cell death in mice. Hence, in the present study we asked whether BIX can prevent such retinal damage. By histologic analysis and TUNEL staining, we estimated that BIX reduced tunicamycin-induced retinal damage in GCL. However, the cell counts in partial cross sections provide a comparatively small sample on which quantitative morphometry can be used to judge such an effect. Therefore, we used Thy-1-CFP transgenic mice[36] to examine the effect of BIX in a large retinal area. This transgene contains a CFP gene under the direction of regulatory elements derived from the mouse Thy-1 gene, and the transgenic mice express CFP protein in RGC and in the inner part of the IPL of the retina.[36] Our results show that BIX exerted a protective effect against tunicamycin-induced retinal damage in the Thy-1-CFP transgenic mouse. However, it is possible that microglial cells become co-labeled with CFP by phagocytosis of the dying RGCs. In this study, we evaluated CFP-positive cells in 7 days after tunicamycin injection. In our previous and preliminary studies, activated microglia cells in GCL were increased at 3 days after NMDA injection[13] and their increases were almost ceased within the 7 days (unpublished data). Furthermore, microglial cells can be distinguished with neuronal cells by their morphologic features.[44] In fact, microglial cells were scarcely observed at seven days after tunicamycin injection, similar to that at seven days after NMDA injection. When we investigated the effect of BIX on NMDA-induced retinal damage in ddY mice, we found that it significantly attenuated such damage. NMDA is well known to induce RGC death and optic-nerve loss (effects mediated by excitatory glutamate receptor), and such neuronal death is believed to play a role in many neurologic and neurodegenerative diseases.[45,46] Recently, Uehara et al.[47] noted that mild exposure to NMDA induced apoptotic cell death in primary cortical culture, and they demonstrated this effect to be caused by an accumulation of polyubiquitinated proteins and increases in XBP-1 mRNA splicing and CHOP mRNA (reflecting activation of the UPR signaling pathway). They also found that protein-disulphide isomerase, which assists in the maturation and transport of unfolded secretory proteins, prevented the neurotoxicity associated with ER stress. These findings suggested that activation of ER stress may participate in the retinal cell death occurring after NMDA-receptor activation and/or an ischemic insult.[47]

In our investigation of the mechanisms underlying the above-mentioned effects, we focused on CHOP. Since CHOP is a member of the CCAAT/enhancer-binding protein family that is induced by ER stress and participates in ER-mediated apoptosis, CHOP may be a key molecule in retinal cell death.[48] We found that treatment with tunicamycin induced apoptotic cell death in RGC-5 and also induced a production of ER stress-related proteins (BiP, the phosphorylated form of eIF2α, and CHOP protein). BIX reduced both the cell death and the CHOP protein expression induced by tunicamycin in RGC-5 in vitro. BIX also attenuated the CHOP protein expression induced by either tunicamycin or NMDA in the mouse retina in vivo. As mentioned above, BIX may affect CHOP protein expression through ATF6 pathway, but no change was observed in BIX-treated RGC-5. In our previous data in SK-N-SH cells, BIX slightly increased CHOP mRNA only at 2 h after the treatment. Expression of CHOP is mainly regulated by three transcription factors—ATF4, cleaved ATF6, and x-box binding protein-1 (XBP-1)—which are downstream effectors during ER stress in similar to other ER chaperones. These differences between BiP and CHOP expression by BIX may be due to the difference of their promoters. CHOP promoter contains at least two ERSE motifs (CHOP ERSE-1 and CHOP ERSE-2) located in opposite directions with a 9 bp overlap, and one of ERSEs is inactive.[49] On the other hand, BiP promoter has three functional ERSE motifs of the rat GRP78 promoter (ERSE-163, ERSE-131, and ERSE-98).[50] These variations in each promoter may contribute to the differences among the expressions of ER chaperons induced by BIX and the lack of CHOP expression.

Subsequently, we monitored XBP-1 activation in the mouse retina in vivo, using ERAI transgenic mice.[37] Effective identification of cells under ER stress conditions is possible in the retina in these mice, as described in our previous report.[13] Here, ERAI mice carrying the F-XBP1ΔDBD-venus expression gene were used to monitor ER stress. The fluorescence intensity arising from the X-box binding protein (XBP1)-venus fusion protein, indicating ER stress activation, was increased in cells within GCL and IPL at 24 h after injection of tunicamycin into the vitreous. BIX significantly reduced this expression, indicating that BIX may attenuate the retinal damage induced

by ER stress-associated factors. In our previous study,[32] we found that BIX induced BiP protein expression via the ATF-6 pathway (not via other ER stress-associated factors such as the PERK and IRE1 pathways) in SK-N-SH cells. Possibly, the protective mechanism underlying the effect of BIX on the mouse retina may be the same as that revealed by our previous study, but further experiments will be needed to clarify this issue.

In conclusion, we have demonstrated that BIX, a preferential inducer of BiP, inhibits both the neuronal cell death induced by ER stress in vitro in RGC-5 cells and in vivo in the mouse retina. Hence, an increase in BiP might be one of the targets of mechanisms bestowing neuroprotection in retinal diseases.

Acknowledgments

The authors thank Masayuki Miura (Department of Genetics, Graduate School of Pharmaceutical Sciences, University of Tokyo, Tokyo, Japan) for the kind gift of ERAI mice, and Rumi Uchibayashi and Shunsake Imai for technical assistance.

References

1. Travers KJ, Patil CK, Wodicka L, Lockhart DJ, Weissman JS, Walter P. Functional and genomic analyses reveal an essential coordination between the unfolded protein response and ER-associated degradation. *Cell.* 2000;101:249–258.
2. Harding HP, Novoa I, Zhang Y, et al. Regulated translation initiation controls stress-induced gene expression in mammalian cells. *Mol Cell.* 2000;6:1099–1108.
3. Schroder M, Kaufman RJ. The mammalian unfolded protein response. *Annu Rev Biochem.* 2005;74:739–789.
4. Katayama T, Imaizumi K, Honda A, et al. Disturbed activation of endoplasmic reticulum stress transducers by familial Alzheimer's disease-linked presenilin-1 mutations. *J Biol Chem.* 2001;276:43446–43454.
5. Ryu EJ, Harding HP, Angelastro JM, Vitolo OV, Ron D, Greene LA. Endoplasmic reticulum stress and the unfolded protein response in cellular models of Parkinson's disease. *J Neurosci.* 2002;22:10690–10698.
6. Oyadomari S, Koizumi A, Takeda K, et al. Targeted disruption of the Chop gene delays endoplasmic reticulum stress-mediated diabetes. *J Clin Invest.* 2002;109:525–532.
7. Roybal CN, Yang S, Sun CW, et al. Homocysteine increases the expression of vascular endothelial growth factor by a mechanism involving endoplasmic reticulum stress and transcription factor ATF4. *J Biol Chem.* 2004;279:14844–14852.
8. Rebello G, Ramesar R, Vorster A, et al. Apoptosis-inducing signal sequence mutation in carbonic anhydrase IV identified in patients with the RP17 form of retinitis pigmentosa. *Proc Natl Acad Sci USA.* 2004;101:6617–6622.
9. Lin JH, Li H, Yasumura D, et al. IRE1 signaling affects cell fate during the unfolded protein response. *Science.* 2007;318:944–949.
10. Joe MK, Sohn S, Hur W, Moon Y, Choi YR, Kee C. Accumulation of mutant myocilins in ER leads to ER stress and potential cytotoxicity in human trabecular meshwork cells. *Biochem Biophys Res Commun.* 2003;312:592–600.
11. Gould DB, Marchant JK, Savinova OV, Smith RS, John SW. Col4a1 mutation causes endoplasmic reticulum stress and genetically modifiable ocular dysgenesis. *Hum Mol Genet.* 2007;16:798–807.
12. Shimazawa M, Ito Y, Inokuchi Y, Hara H. Involvement of double-stranded RNA-dependent protein kinase in ER stress-induced retinal neuron damage. *Invest Ophthalmol Vis Sci.* 2007;48:3729–3736.
13. Shimazawa M, Inokuchi Y, Ito Y, et al. Involvement of ER stress in retinal cell death. *Mol Vis.* 2007;13:578–587.
14. Mahoney WC, Duksin D. Biological activities of the two major components of tunicamycin. *J Biol Chem.* 1979;254:6572–6576.
15. Awai M, Koga T, Inomata Y, et al. NMDA-induced retinal injury is mediated by an endoplasmic reticulum stress-related protein, CHOP/GADD153. *J Neurochem.* 2006;96:43–52.
16. Lee YK, Brewer JW, Hellman R, Hendershot LM. BiP and immunoglobulin light chain cooperate to control the folding of heavy chain and ensure the fidelity of immunoglobulin assembly. *Mol Biol Cell.* 1999;10:2209–2219.
17. Li WW, Alexandre S, Cao X, Lee AS. Transactivation of the grp78 promoter by Ca^{2+} depletion. A comparative analysis with A23187 and the endoplasmic reticulum Ca^{2+}-ATPase inhibitor thapsigargin. *J Biol Chem.* 1993;268:12003–12009.
18. van de Put FH, Elliott AC. The endoplasmic reticulum can act as a functional Ca^{2+} store in all subcellular regions of the pancreatic acinar cell. *J Biol Chem.* 1997;272:27764–27770.
19. Lievremont JP, Rizzuto R, Hendershot L, Meldolesi J. BiP, a major chaperone protein of the endoplasmic reticulum lumen, plays a direct and important role in the storage of the rapidly exchanging pool of Ca^{2+}. *J Biol Chem.* 1997;272:30873–30879.
20. Helenius A. How N-linked oligosaccharides affect glycoprotein folding in the endoplasmic reticulum. *Mol Biol Cell.* 1994;5:253–265.
21. Kuznetsov G, Chen LB, Nigam SK. Multiple molecular chaperones complex with misfolded large oligomeric glycoproteins in the endoplasmic reticulum. *J Biol Chem.* 1997;272:3057–3063.
22. Klausner RD, Sitia R. Protein degradation in the endoplasmic reticulum. *Cell.* 1990;62:611–614.
23. Blond-Elguindi S, Cwirla SE, Dower WJ, et al. Affinity panning of a library of peptides displayed on bacteriophages reveals the binding specificity of BiP. *Cell.* 1993;75:717–728.
24. Knarr G, Gething MJ, Modrow S, Buchner J. BiP binding sequences in antibodies. *J Biol Chem.* 1995;270:27589–27594.
25. Knarr G, Modrow S, Todd A, Gething MJ, Buchner J. BiP-binding sequences in HIV gp160. Implications for the binding specificity of bip. *J Biol Chem.* 1999;274:29850–29857.
26. Brodsky JL, Werner ED, Dubas ME, Goeckeler JL, Kruse KB, McCracken AA. The requirement for molecular chaperones during endoplasmic reticulum-associated protein degradation demonstrates that protein export and import are mechanistically distinct. *J Biol Chem.* 1999;274:3453–3460.
27. Meerovitch K, Wing S, Goltzman D. Proparathyroid hormone-related protein is associated with the chaperone protein BiP and undergoes proteasome-mediated degradation. *J Biol Chem.* 1998;273:21025–21030.
28. Katayama T, Imaizumi K, Sato N, et al. Presenilin-1 mutations downregulate the signalling pathway of the unfolded-protein response. *Nat Cell Biol.* 1999;1:479–485.
29. Yu Z, Luo H, Fu W, Mattson MP. The endoplasmic reticulum stress-responsive protein GRP78 protects neurons against excitotoxicity and apoptosis: suppression of oxidative stress and stabilization of calcium homeostasis. *Exp Neurol.* 1999;155:302–314.
30. Rao RV, Peel A, Logvinova A, et al. Coupling endoplasmic reticulum stress to the cell death program: role of the ER chaperone GRP78. *FEBS Lett.* 2002;514:122–128.
31. Reddy RK, Mao C, Baumeister P, Austin RC, Kaufman RJ, Lee AS. Endoplasmic reticulum chaperone protein GRP78 protects cells from apoptosis induced by topoisomerase inhibitors: role of ATP binding site in suppression of caspase-7 activation. *J Biol Chem.* 2003;278:20915–20924.
32. Kudo T, Kanemoto S, Hara H, et al. A molecular chaperone inducer protects neurons from ER stress. *Cell Death Differ.* 2008;15:364–375.
33. Krishnamoorthy RR, Agarwal P, Prasanna G, et al. Characterization of a transformed rat retinal ganglion cell line. *Brain Res Mol Brain Res.* 2001;86:1–12.
34. Chen D, Padiernos E, Ding F, Lossos IS, Lopez CD. Apoptosis-stimulating protein of p53–2 (ASPP2/53BP2L) is an E2F target gene. *Cell Death Differ.* 2005;12:358–368.
35. Jiang Y, Ahn EY, Ryu SH, et al. Cytotoxicity of psammaplin A from a two-sponge association may correlate with the inhibition of DNA replication. *BMC Cancer.* 2004;4:70.
36. Feng G, Mellor RH, Bernstein M, et al. Imaging neuronal subsets in transgenic mice expressing multiple spectral variants of GFP. *Neuron.* 2000;28:41–51.
37. Iwawaki T, Akai R, Kohno K, Miura M. A transgenic mouse model for monitoring endoplasmic reticulum stress. *Nat Med.* 2004;10:98–102.